

# A Map of the Universe

J. Richard Gott, III,<sup>1</sup> Mario Jurić,<sup>1</sup> David Schlegel,<sup>1</sup> Fiona Hoyle,<sup>2</sup> Michael Vogeley,<sup>2</sup>  
Max Tegmark,<sup>3</sup> Neta Bahcall,<sup>1</sup> Jon Brinkmann<sup>4</sup>

## ABSTRACT

We have produced a new conformal map of the universe illustrating recent discoveries, ranging from Kuiper belt objects in the Solar system, to the galaxies and quasars from the Sloan Digital Sky Survey. This map projection, based on the logarithm map of the complex plane, preserves shapes locally, and yet is able to display the entire range of astronomical scales from the Earth's neighborhood to the cosmic microwave background. The conformal nature of the projection, preserving shapes locally, may be of particular use for analyzing large scale structure. Prominent in the map is a Sloan Great Wall of galaxies 1.37 billion light years long, 80% longer than the Great Wall discovered by Geller and Huchra and therefore the largest observed structure in the universe.

*Subject headings:* methods: data analysis, large-scale structure of universe

## 1. Introduction

Cartographers mapping the Earth's surface were faced with the challenge of mapping a curved surface onto a plane. No such projection can be perfect, but it can capture important features. Perhaps the most famous map projection is the Mercator projection (presented by Gerhardus Mercator in 1569). This is a conformal projection which preserves shapes locally. Lines of latitude are shown as straight horizontal lines, while meridians of longitude are shown as straight vertical lines. If the Mercator projection is plotted on an  $(x, y)$  plane, the coordinates are plotted as follows:  $x = \lambda$ , and  $y = \ln(\tan(\pi/4 + \phi/2))$  where  $\phi$  (positive if north, negative if south) is the latitude in radians, while  $\lambda$  (positive if easterly, negative if westerly) is the longitude in radians (see Snyder (1993) for an excellent discussion of this and

<sup>1</sup>Department of Astrophysical Sciences, Princeton University, Princeton, NJ 08544

<sup>2</sup>Department of Physics, Drexel University, Philadelphia, PA 19104

<sup>3</sup>Department of Physics, University of Pennsylvania, Philadelphia, PA 19104

<sup>4</sup>Apache Point Observatory, 2001 Apache Point Road, P.O Box 59,Sunspot, NM, 88349

other map projections of the Earth.) This conformal map projection preserves angles locally, and also compass directions. Local shapes are good, while the scale varies as a function of latitude. Thus, the shapes of both Iceland and South America are shown well, although Iceland is shown larger than it should be relative to South America. Other map projections preserve other properties. The stereographic projection which, like the Mercator projection, is conformal is often used to map hemispheres. The gnomonic map projection (effectively from a "light" at the center of the globe onto a tangent plane) maps geodesics into straight lines on the flat map, but does not preserve shapes or areas. Equal area map projections like the Lambert, Mollweide, and Hammer projections preserve areas but not shapes.

A Lambert azimuthal equal area projection, centered on the north pole has in polar coordinates  $(r, \theta)$ ,  $\theta = \lambda$ ,  $r = 2r_0 \sin[(\pi/2 - \phi)/2]$ , where  $r_0$  is the radius of the sphere. This projection preserves areas. The northern hemisphere is thus mapped onto a circular disk of radius  $\sqrt{2}r_0$  and area  $2\pi r_0^2$ . An oblique version of this, centered at a point on the equator, is also possible.

The Hammer projection shows the Earth as a horizontal ellipse with 2:1 axis ratio. The equator is shown as a straight horizontal line marking the long axis of the ellipse. It is produced in the following way: map the entire sphere onto its western hemisphere by simply compressing each longitude by a factor of 2. Now map this western hemisphere onto a plane by the Lambert equal area azimuthal projection. This map is a circular disk. This is then stretched by a factor of 2 (undoing the previous compression by a factor of 2) in the equatorial direction to make an ellipse with a 2:1 axis ratio. Thus, the Hammer projection preserves areas. The Mollweide projection also shows the sphere as 2:1 axis ratio ellipse.  $(x, y)$  coordinates on the map are:  $x = (2\sqrt{2}/\pi)r_0\lambda \cos \theta$ , and  $y = \sqrt{2}r_0 \sin \theta$  where  $2\theta + \sin 2\theta = \pi \sin \phi$ . This projection is equal area as well. Latitude lines on the Mollweide projection are straight, whereas they are curved arcs on the Hammer projection.

Astronomers mapping the sky have also used such map projections of the sphere. Gnomonic maps of the celestial sphere onto a cube date from 1674. In recent times, Turner and Gott (1976) used the stereographic map projection to chart groups of galaxies (utilizing its property of mapping circles in the sky onto circles on the map.) The COBE satellite map (Smoot et al. (1992)) of the cosmic microwave background used an equal area map projection of the celestial sphere onto a cube. The WMAP satellite (Bennett et al. (2003)) mapped the celestial sphere onto a rhombic dodecahedron using the Healpix equal area map projection (Górski et al. (1999)). Its results were displayed also on the Mollweide map projection, showing the celestial sphere as an ellipse, which was chosen for its equal area property, and the fact that lines of constant galactic latitude are shown as straight lines.

de Lapparent, Geller, & Huchra (1986) pioneered use of slice maps of the universe to

make flat maps. They surveyed a slice of sky,  $117^\circ$  long and  $6^\circ$  wide, of constant declination. In 3D this slice had the geometry of a cone, and they flattened this onto a plane. (A cone has zero Gaussian curvature and can therefore be constructed from a piece of paper. A cone cut along a line and flattened onto a plane looks like a pizza with a slice missing.) If the cone is at declination  $\delta$ , the map in the plane will be  $x = r \cos(\lambda \cos(\delta))$ ,  $y = r \sin(\lambda \cos(\delta))$ , where  $\lambda$  is the right ascension (in radians), and  $r$  is the co-moving distance (as indicated by the redshift of the object). This will preserve shapes. Many times a  $360^\circ$  slice is shown as a circle with the Earth in the center, where  $x = r \cos(\lambda)$ ,  $y = r \sin(\lambda)$ . If  $r$  is measured in co-moving distance, this will preserve shapes only if the universe is flat ( $k = 0$ ), and the slice is in the equatorial plane ( $\delta = 0$ ), (if  $\delta \neq 0$ , structures (such as voids) will appear lengthened in the direction tangential to the line of sight by a factor of  $1/\cos(\delta)$ ). This correction is important for study of the Alcock-Paczynski effect, which says that structures such as voids will not be shown in proper shape if we take simply  $r = z$  (Alcock and Paczynski (1979)). In fact, Ryden (1995) and Ryden & Melott (1996) have emphasized that this shape distortion in redshift space can be used to test the cosmological model in a large sample such as the Sloan Digital Sky Survey (York et al. (2000); Gunn et al. (1998); Fukugita et al. (1996)). If voids run into each other, the walls will on average not have systematic peculiar velocities and therefore voids should have approximately round shapes (a proposition which can be checked in detail with N-body simulations). Therefore, it is important to investigate map projections which will preserve shapes locally. If one has the correct cosmological model, and uses such a conformal map projection, isotropic features in the large scale structure will appear isotropic on the map.

Astronomers mapping the universe are confronted with the challenge of showing a wide variety of scales. What should a map of the universe show? It should show locations of all the famous things in space: the Hubble Space Telescope, the International Space Station, other satellites orbiting the Earth, the van Allen radiation belts, the Moon, the Sun, planets, asteroids, Kuiper belt objects, nearby stars such as  $\alpha$  Centauri, and Sirius, stars with planets such as 51 Peg, stars in our galaxy, famous black holes and pulsars, the galactic center, Large and Small Magellanic Clouds, M31, famous galaxies like M87, the Great Wall, famous quasars like 3C273 (Schmidt (1963)) and the gravitationally lensed quasar 0957 (Kundic et al. (1997)), distant Sloan Digital Sky Survey galaxies, and quasars, the most distant known quasar and galaxy and finally the cosmic microwave background radiation. This is quite a challenge. Perhaps the first book to address this challenge was Cosmic View: The Universe in 40 Jumps by Kees Boeke published in 1957 (Boeke (1957)). This brilliant book started with a picture of a little girl shown at 1/10th scale. The next picture showed the same little girl at 1/100th scale who now could be seen sitting in her school courtyard. Each successive picture was plotted at ten times smaller scale. The 8th

picture, at a scale of  $1/10^8$ , shows the entire Earth. The 14th picture, at a scale of  $1/10^{14}$ , shows the entire Solar system. The 18th picture, at a scale of  $1/10^{18}$ , includes  $\alpha$  Centauri. The 22<sup>nd</sup> picture, at a scale of  $1/10^{22}$  shows all of the Milky Way Galaxy. The 26<sup>th</sup> and last picture in the sequence shows galaxies out to a distance of 750 million light years. A further sequence of pictures labeled  $0, -1, -2, \dots - 13$ , starting with a life size picture of the girl's hand, shows a sequence of microscopic views, each ten times larger in size, ending with a view of the nucleus of a sodium atom at a scale of  $10^{13}/1$ . A modern version of this book, Powers of Ten (Morrison et al. (1982)) by Phillip and Phylis Morrison and the Office of Charles & Ray Eames, is probably familiar to most astronomers. This successfully addresses the scale problem, but is an atlas of maps, not a single map. How does one show the entire observable universe in a single map?

The modern Powers of Ten book described above is based on a movie, Powers of Ten (Eames and Eames (1977)), by Charles and Ray Eames which in turn was inspired by Kees Boeke's book. The movie is arguably an even more brilliant presentation than Kees Boeke's original book. The camera starts with a picture of a couple sitting on a picnic blanket in Chicago, and then the camera moves outward, increasing its distance from them exponentially as a function of time. Thus, approximately every ten seconds, the view is from ten times further away and corresponds to the next picture in the book. The movie gives one long continuous shot, which is breathtaking as it moves out. The movie is called Powers of Ten (and recently, an IMAX version of this idea has been made, called "Cosmic Voyage"), but it could equally well be titled Powers of Two, or Powers of  $e$ , because its exponential change of scale with time, produces a reduction by a factor of two in constant time intervals, and also a factor of  $e$  in constant time intervals. The time intervals between factors of 10, factors of 2 and factors of  $e$  in the movie are related by the ratios  $\ln 10 : \ln 2 : 1$ . Still, this is not a single map which can be studied all at once, or which can be hung on a wall.

We want to see the large scale structure of galaxy clustering but are also interested in stars in our own galaxy and the Moon and planets. Objects close to us may be inconsequential in terms of the whole universe but they are important to us. It reminds one of the famous cartoon New Yorker cover "View of the World from 9<sup>th</sup> Avenue" by Saul Steinberg of May 29, 1976 (Steinberg (1976)). It humorously shows a New Yorker's view of the world. The traffic, sidewalks and buildings along 9<sup>th</sup> Avenue are visible in the foreground. Behind is the Hudson river, with New Jersey as a thin strip on the far bank. Then at even smaller scale is the rest of the United States with the Rocky mountains sticking up like small hills. In the background, but not much wider than the Hudson River, is the entire Pacific ocean with China and Japan in the distance. This is, of course a parochial view, but it is just that kind of view that we want of the universe. We would like a single map that would equally well

show both interesting objects in the solar system, nearby stars, galaxies in the Local Group, and large scale structure out to the cosmic microwave background.

## 2. Co-moving coordinates

Our objective here is to produce a conformal map of the universe which will show the wide range of scales encountered while still showing shapes that are locally correct.

Consider the general Friedmann metrics:

$$ds^2 = -dt^2 + a^2(t)(d\chi^2 + \sin^2 \chi(d\theta^2 + \sin^2 \theta d\phi^2)), \quad k = +1 \quad (1)$$

$$ds^2 = -dt^2 + a^2(t)(d\chi^2 + \chi^2(d\theta^2 + \sin^2 \theta d\phi^2)), \quad k = 0 \quad (2)$$

$$ds^2 = -dt^2 + a^2(t)(d\chi^2 + \sinh^2 \chi(d\theta^2 + \sin^2 \theta d\phi^2)), \quad k = -1 \quad (3)$$

where  $t$  is the cosmic time since the Big Bang,  $a(t)$  is the expansion parameter, and individual galaxies participating in the cosmic expansion follow geodesics with constant values of  $\chi$ ,  $\theta$ , and  $\phi$ . These three are called co-moving coordinates. Neglecting peculiar velocities, galaxies remain at constant positions in co-moving coordinates as the universe expands. Now  $a(t)$  obeys Friedmann's equations:

$$\left(\frac{a_{,t}}{a}\right)^2 = -\frac{k}{a^2} + \frac{\Lambda}{3} + \frac{8\pi\rho_m}{3} + \frac{8\pi\rho_r}{3} \quad (4)$$

$$2\left(\frac{a_{,tt}}{a}\right) = \frac{2\Lambda}{3} - \frac{8\pi\rho_m}{3} - \frac{16\pi\rho_r}{3} \quad (5)$$

where  $\Lambda = const.$ , is the cosmological constant,  $\rho_m \propto a^{-3}$ , is the average matter density in the universe, including cold dark matter,  $\rho_r \propto a^{-4}$  is the average radiation density in the universe, primarily the cosmic microwave background radiation. The second equation shows that the cosmological constant produces an acceleration in the expansion while the matter and radiation produce a deceleration. Per unit mass density, radiation produces twice the deceleration of normal matter because positive pressure is gravitationally attractive in Einstein's theory and radiation has a pressure in each of the three directions ( $x, y, z$ ) which is  $1/3^{rd}$  the energy density.

We can define a conformal time  $\eta$  by the relation  $d\eta = dt/a$ , so that

$$\eta(t) = \int_0^t \frac{dt}{a} \quad (6)$$

Light travels on radial geodesics with  $d\eta = \pm d\chi$  so a galaxy at a co-moving distance  $\chi$  from us emitted the light we see today at a conformal time  $\eta(t) = \eta(t_0) - \chi$ . Thus, we

can calculate the time  $t$  and redshift  $z = a(t_0)/a(t) - 1$  at which that light was emitted. Conversely, if we know the redshift, given a cosmological model (i.e. values of  $H_0$ ,  $\Lambda$ ,  $\rho_m$ ,  $\rho_r$ , and  $k$  today) we can calculate the co-moving radial distance of the galaxy from us from its redshift, again ignoring peculiar velocities. For a more detailed discussion of distance measures in cosmology, see Hogg (1999).

The WMAP satellite has measured the cosmic microwave background in exquisite detail (Bennett et al. (2003)) and combined this data with other data (Percival et al. (2001); Verde et al. (2002); Croft et al. (2002); Gnedin & Hamilton (2002); Garnavich et al. (1998); Riess et al. (2001); Freedman et al. (2001); Perlmutter et al. (1999)) to produce accurate data on the cosmological model (Spergel et al. (2003)). We adopt best fit values at the present epoch,  $t = t_0$ , based on the WMAP data of:

$$\begin{aligned} H_0 &\equiv \frac{a,t}{a} = 71 \frac{\text{km}}{\text{sec Mpc}}, \\ \Omega_\Lambda &\equiv \frac{\Lambda}{3H_0^2} = 0.73, \\ \Omega_r &= 8.35 \cdot 10^{-5}, \\ \Omega_m &\equiv \frac{8\pi\rho_m}{3H_0^2} = 0.27 - \Omega_r, \\ k &= 0. \end{aligned}$$

The WMAP data implies that  $w \approx -1$  for dark energy (ie.  $p_{vac} = w\rho_{vac} \approx -\rho_{vac}$ ), suggesting that a cosmological constant is an excellent model for the dark energy, so we are simply adopting that. The current Hubble radius  $R_{H_0} = cH_0^{-1} = 4220$  Mpc. The cosmic microwave background is at a redshift  $z = 1089$ . Substituting, using geometrized units in which  $c = 1$ , and integrating the first Friedmann equation we find the conformal time may be calculated:

$$\eta(t) = \int_0^t \frac{dt}{a} = \int_0^{a(t)} \left\{ -ka^2 + \frac{8\pi}{3}a^4[\rho_m(a) + \rho_r(a)] + \frac{\Lambda}{3}a^4 \right\}^{-1/2} da \quad (7)$$

where  $\rho_m \propto a^{-3}$  and  $\rho_r \propto a^{-4}$ . This formula will accurately track the value of  $\eta(t)$ , providing that this is interpreted as the value of the conformal time since the end of the inflationary period at the beginning of the universe. (During the inflationary period at the beginning of the universe, the cosmological constant assumed a large value, different from that observed today, and the formula would have to be changed accordingly. So we simply start the clock at the end of the inflationary period where the energy density in the false vacuum [large cosmological constant] is dumped in the form of matter and radiation. Thus, when we trace back to the big bang, we are really tracing back to the end of the inflationary period. After that, the model does behave just like a standard hot-Friedmann big bang model. This standard model might be properly referred to as an inflationary-big bang model, with the

inflationary epoch producing the Big Bang explosion at the start.) Now,  $a(t)$  is the radius of curvature of the universe for the  $k = +1$  and  $k = -1$  cases, but for the  $k = 0$  case, which we will be investigating first and primarily, there is no scale and so we are free to normalize, setting  $a(t_0) = R_{H_0} = cH_0^{-1} = 4220 \text{ Mpc}$ . Then,  $\chi$  measures co-moving distances at the present epoch in units of the current Hubble radius  $R_{H_0}$ . Thus, for the  $k = 0$  case, using geometrized units, we have:

$$\eta(a) = \eta(a(t)) = \int_0^a \left( \frac{a}{a_0} \Omega_m + \Omega_r + \left( \frac{a}{a_0} \right)^4 \Omega_\Lambda \right)^{-1/2} \frac{da}{a_0} \quad (8)$$

where  $\Omega_m$ ,  $\Omega_\Lambda$ ,  $\Omega_r$  are the values at the current epoch. Given the values adopted from WMAP we find:

$$\eta(a_0) = 3.38 \quad (9)$$

That means that when we look out now at  $t = t_0$  (when  $a = a_0$ ) we can see out to a distance of

$$\chi = 3.38 \quad (10)$$

or a co-moving distance of

$$\chi R_{H_0} = 3.38 R_{H_0} = 14,300 \text{ Mpc}. \quad (11)$$

This is the effective particle horizon, where we are seeing particles at the moment of the Big Bang. This is a larger radius than 13.7 billion light years – the age of the universe (the lookback time) times the speed of light – because it shows the co-moving distance the most distant particles we can observe now will have from us when they are as old as we are now, i.e. measured at the current cosmological epoch. We may calculate the value of  $\eta$  as a function of  $a$ , or equivalently as a function of observed redshift  $z = (a_0/a) - 1$ . Recombination occurs at  $z_{rec} = 1089$ , which is the redshift of the cosmic microwave background seen by WMAP.

$$\eta(z_{rec}) = 0.0671 \quad (12)$$

So, the co-moving radius of the cosmic microwave background is:

$$\chi R_{H_0} = (\eta_0 - \eta_{rec}) R_{H_0} = 14,000 \text{ Mpc} \quad (13)$$

That is the radius at the current epoch, so at recombination the WMAP sphere has a physical radius that is 1090 times smaller or about 13 Mpc.

According to SDSS luminosity function data (Michael Blanton, private communication),  $L_*$  in the Press and Schechter luminosity function in B band is  $7.1 \cdot 10^9 L_\odot$  for  $H_0 = 71 \text{ km/s Mpc}^{-1}$  and the mean separation between galaxies brighter than  $L_*$  is 4.1 Mpc. The Milky Way has  $9.4 \cdot 10^9 L_\odot$  in B. Since the radius of the observable universe (out to the

cosmic microwave background) is 14 Gpc, that means that the number of bright galaxies (more luminous than  $L_*$ ) forming within the currently observable universe is of order 170 billion. If our galaxy has of order 200 billion stars, the mean blue stellar luminosity is of order  $0.05 L_\odot$  and the mean number density of stars is at least of order  $2.6 \cdot 10^9 \text{Mpc}^{-3}$ . Ellipticals and S0 galaxies have a higher number of stars per Solar luminosity than the Milky Way, so a conservative estimate for the mean number density of stars might be  $5 \cdot 10^9 \text{ stars/Mpc}^3$ . Thus, the currently observable universe is home to of order  $6 \cdot 10^{22}$  stars.

We may compute co-moving radii  $r = \chi R_{H_0}$  for different redshifts, as shown in table 1. We can also calculate the value of  $\eta(t = \infty) = 4.50$  which shows how far a photon can travel in co-moving coordinates from the inflationary Big Bang to the infinite future. Thus, if we wait until the infinite future we will eventually be able to see out to a co-moving distance of

$$r_{t=\infty} = 4.50R_{H_0} = 19,000 \text{ Mpc} \quad (14)$$

This is the co-moving future visibility limit. No matter how long we wait, we will not be able to see further than this. This is surprisingly close. The number of galaxies we will eventually ever be able to see is only larger than number observable today by a factor of  $(r_{t=\infty}/r_{t_0})^3 = 2.36$ .

This calculation assumes the false vacuum state (cosmological constant) visible today remains unchanged. (The WMAP data is consistent with a value of  $w = -1$ , indicating that the vacuum state (dark energy) today is well approximated by a positive cosmological constant. This false vacuum state (with  $p_{vac} = w\rho_{vac} = -1\rho_{vac}$ ) may decay by forming bubbles of normal zero density vacuum ( $\Lambda = 0$ ) or even decay by forming bubbles of negative energy density vacuum ( $\Lambda < 0$ ). If the present false vacuum is only metastable it will eventually decay by the formation of bubbles of normal or negative energy density vacuum and eventually one of these bubbles will engulf the co-moving location of our galaxy. But if these bubbles occur late ( $> 10^{100}$  yrs) as expected they will make a negligible correction to how far away in comoving coordinates we will eventually be able to see. For a fuller discussion, see Gott, Jurić et al. (astro-ph/0310571v1) and references therein.

Linde (1990) and Garriga and Vilenkin (1998) have pointed out that if the current vacuum state is the lowest stable equilibrium then quantum fluctuations can form bubbles of high density vacuum that will start a new inflationary epoch, new baby universes growing like branches off a tree. Still, as in the above case, we expect to be engulfed by such a new inflating region only at late times (say at least  $10^{100}$  years from now) and the observer will still be surrounded by an event horizon with a limit of future visibility in co-moving coordinates in our universe that is virtually identical with what we have plotted. Thus, although the future history of the universe will be determined by the subsequent evolution of the quantum vacuum state (as also noted by Krauss & Starkman (2000)), in practice we

expect the current vacuum to stay as is for considerably longer than the Hubble time, and in many scenarios this leaves us with a limit of future visibility that is for all practical purposes just what we have plotted.

If we send out a light signal now, by  $t = \infty$  it will reach a radius  $\chi = \eta(t = \infty) - \eta(t_0) = 4.50 - 3.38 = 1.12$ , or

$$r = 4,740 \text{ Mpc} \quad (15)$$

to which we refer to as the “outward limit of reachability”. We cannot reach (with light signals or rockets) any galaxies that are further away than this (Busha et al. (2003)). What redshift does this correspond to? Galaxies we observe today with a redshift of  $z = 1.69$  are at this co-moving distance. Galaxies with redshifts larger than 1.69 today are unreachable. This is a surprisingly small redshift.

We can see many galaxies at redshifts larger than 1.69 that we will never be able to visit or signal. In the accelerating universe, these galaxies are accelerating away from us so fast that we can never catch them. The total number of stars that our radio signals will ever pass is of order  $2 \times 10^{21}$ .

### 3. A Map Projection for the Universe

We will choose a conformal map that will cover the wide range of scales from the Earth’s neighborhood to the cosmic microwave background. First we will consider the flat case ( $k = 0$ ) which the WMAP data tells us is the appropriate cosmological model. Our map will be two dimensional so that it can be shown on a wall chart. de Lapparent, Geller, & Huchra (1986) showed with their slice of the universe, just how successful a slice of the universe can be in illustrating large scale structure. The Sloan Digital Survey should eventually include spectra and accurate positions for about 1 million galaxies and quasars in a 3D sample (see Stoughton et al. (2002); Abazajian et al. (2003); Strauss et al. (2002); Richards et al. (2002); Eisenstein et al. (2001) for SDSS scientific results and Blanton et al. (2003); Hogg et al. (2003); Smith et al. (2002); Pier et al. (2003) for further technical reference). But virtually complete already is an equatorial slice 4 degrees wide ( $-2^\circ < \delta < 2^\circ$ ) centered on the celestial equator covering both northern and southern galactic hemispheres. This shows many interesting features including many prominent voids and a great wall longer than the great wall found by Geller and Huchra (1989).

Since the observed slice is already in a flat plane ( $k = 0$  model, along the celestial equator) we may project this slice directly onto a flat sheet of paper using polar coordinates with  $r = \chi R_{H_0}$  being the co-moving distance, and  $\theta$  being the right ascension. (CMB

observations from Boomerang, DASI, MAXIMA and WMAP indicate that the case  $k = 0$  is the appropriate one for the universe. For mathematical completeness we will also consider the  $k = +1$  and  $k = -1$  cases in an appendix.) We wish to show large scale structure and the extent of the observable universe out to the cosmic microwave background radiation including all the SDSS galaxies and quasars in the equatorial slice. In figure 1, one can see the cosmic microwave background at the surface of last scattering as a circle. Its co-moving radius is 14.0 Gpc. (Since the size of the universe at the epoch of recombination is smaller than that at present by a factor of  $1 + z = 1090$ , the true radius of this circle is about 12.84 Mpc.) Slightly beyond the cosmic microwave background in co-moving coordinates is the Big Bang at a co-moving distance of 14.3 Gpc.

(Imagine a point on the cosmic microwave background circle. Draw a radius around that point that is tangent to the outer circle labeled Big Bang, as shown in the figure, in other words, a circle that has a radius equal to the difference in radius between the cosmic microwave background circle and the Big Bang circle. That circle has a co-moving radius of 283 Mpc. That is the co-moving horizon radius at recombination. If the Big Bang model – without inflation – were correct we would expect a point on the cosmic microwave background circle to be causally influenced only by things inside that horizon radius at recombination. The angular radius of this small circle as seen from the Earth is  $(283 \text{ Mpc}/14,000 \text{ Mpc})$  radians or  $1.16^\circ$ . If the Big Bang model without inflation were correct we would expect the cosmic microwave background to be correlated on scales of at most  $1.16^\circ$ . Inflation, by having a short period of accelerated expansion during the first  $10^{-34}$  seconds of the universe, puts distant regions in causal contact because of the slight additional time allowed when the universe was very small. So, with inflation, we can understand why the cosmic microwave background is uniform to one part in 100,000 all over the sky. Furthermore, random quantum fluctuations predicted by inflation add a series of adiabatic fluctuations which are expected to have a peak in the power spectrum at an angular scale about the size of the horizon radius at recombination calculated above,  $\sim 0.86$  degrees.)

Beyond the Big Bang circle is the circle showing the future co-moving visibility limit. If we wait until the infinite future, we will be able to see out to this circle. (In other words, in the infinite future, we will be able to see particles at the future co-moving visibility limit as they appeared at the Big Bang.)

The SDSS quasars extend out about halfway out to the cosmic microwave background radiation. The distribution of quasars shows several features. The radial distribution shows several shelves due to selection effects as different spectral features used to identify quasars come into view in the visible. Several radial spokes appear due to incompleteness in some narrow right ascension intervals. Two large fan shaped regions are empty and not surveyed

because they cover the zone of avoidance close to the galactic plane which is not included in the Sloan survey. These excluded regions run from approximately  $3.7 \text{ h} \lesssim \alpha \lesssim 8.7 \text{ h}$  and approximately  $16.7 \text{ h} \lesssim \alpha \lesssim 20.7 \text{ h}$ . The quasars do not show noticeable clustering or large scale structure. This is because the quasars are so widely spaced that the mean distance between quasars is larger than the correlation length at that epoch.

The circle of reachability is also shown. Quasars beyond this circle are unreachable. Radio signals emitted by us now will only reach out as far as this circle, even in the infinite future.

The SDSS galaxies appear as a black blob in the center. There is much interesting large scale structure here but the field is too crowded and small to show it. This illustrates the problem of scale in depicting the universe. If we want a map of the entire observable universe on one page, at a nice scale, the galaxies are crammed into a blob in the center. Let us enlarge the central circle of radius 0.06 times the distance to the Big Bang circle by a factor of 16.6 and plot it again in figure 2. This now shows a circle of co-moving radius 858 Mpc. Almost all of these points are galaxies from the galaxy and bright red galaxy samples of the SDSS. Now we can see a lot of interesting structure. The most prominent feature is a Sloan Great Wall at a median distance of about 310 Mpc stretching from 8.7h to 14h in R.A. There are numerous voids. A particularly interesting one is close in at a co-moving distance of 125 Mpc at 1.5h R.A. At the far end of this void are a couple of prominent clusters of galaxies which are recognizable as "fingers of God" pointing at the Earth. Redshift in this map is taken as the co-moving distance indicator assuming participation in the Hubble flow, but galaxies also have peculiar velocities and in a dense cluster with a high velocity dispersion this causes the distance errors due to these peculiar velocities to spread the galaxy positions out in the radial direction producing the "finger of God" pointing at the Earth. Numerous other clusters can be similarly identified. This is a conformal map, that preserves shapes – excluding the small effects of peculiar velocities. The original CfA survey in which Geller and Huchra discovered the Great Wall had a co-moving radius of only 211 Mpc, which is less than a quarter of the radius shown in figure 2. Figure 2 is a quite impressive picture, but it does not capture all of the Sloan Survey. If we displayed figure 1 at a scale enlarged by a factor of 16.6 the central portion of the map would be as you see displayed at the scale shown in figure 2 which is adequate, but the Big Bang circle would have a diameter of 6.75 feet. You could put this on your wall, but if we were to print it in the journal for you to assemble it would require the next 256 pages. This points out the problem of scale for even showing the Sloan Survey all on one page. Small scales are also not represented well. The distance to the Virgo Cluster in figure 2 is only about 2 mm and the distance from the Milky Way to M31 is only 1/13th of a millimeter and therefore invisible on this Map. Figure 2, dramatic as it is, fails to capture a picture of all the external galaxies and quasars. The nearby galaxies

are too close to see and the quasars are beyond the limits of the page.

We may try plotting the universe in lookback time rather than co-moving coordinates. The result is in figure 3. The outer circle is the cosmic microwave background. It is indistinguishable from the Big Bang as the two are separated by only 380,000 years out of 13.7 billion years. The SDSS quasars now extend back nearly to the cosmic microwave background radiation (since it is true that we are seeing back to within a billion years of the Big Bang). Lookback time is easier to explain to a lay audience than co-moving coordinates and it makes the SDSS data look more impressive, but it is a misleading portrayal as far as shapes and the geometry of space are concerned. It misleads us as to how far out we are seeing in space. For that, co-moving coordinates are appropriate. figure 3 does not preserve shapes – it compresses the large area between the SDSS quasars and the cosmic microwave background into a thin rim. This is not a conformal map. The SDSS galaxies now occupy a larger space in the center, but they are still so crowded together that one can not see the large scale structure clearly. Figure 4 shows the central 0.2 radius circle (shown as a dotted circle in figure 3) enlarged by a factor of 5. Thus if we were to make a wall map of the observable universe using lookback time at the scale of figure 4 it would only need to be 2 feet across and would only require the next 25 pages in the journal to plot. This is an advantage of the lookback time map. It makes the interesting large scale structure that we see locally (figure 4) a factor of slightly over 3 larger in size relative to the cosmic microwave background circle than if we had used co-moving coordinates. Figure 4 looks quite similar to figure 2. At co-moving radii less than 858 Mpc, the lookback time and co-moving radius are rather similar. Still, figure 4 is not perfectly conformal. Near the outer edges there is a slight radial compression that is beginning to occur in the lookback time map as one goes toward the Big Bang. The effects of radial compression are illustrated in figure 5, where we have plotted a square grid in co-moving coordinates in terms of lookback time as would be depicted in figure 3. Each grid square would contain an equal number of galaxies in a flat slice of constant vertical thickness. This shows the distortion of space that is produced by using the lookback time. The squares become more and more distorted in shape as one approaches the edge.

Thus, it would be useful to have a conformal map projection that would show the whole SDSS survey, including galaxies, quasars and the cosmic microwave background, as well as smaller scales, covering the local supercluster, the Local Group, the Milky Way, nearby stars, the Sun and planets, the Moon and artificial Earth satellites. Such a map is possible.

Consider the complex plane  $(u, v) = u + iv$  where  $i = \sqrt{-1}$  and  $u$  and  $v$  are real numbers. Every complex number  $W = u + iv$  will be represented as a point in the  $(u, v)$  plane where  $u$  and  $v$  are the usual Cartesian coordinates. The function  $Z = i \ln(W)$  maps the plane  $(u, v)$

onto the plane  $(x, y)$  where  $Z = x + iy$ . The  $(u, v)$  plane represents a slice of the universe in isotropic coordinates (in this case co-moving coordinates since  $k = 0$ ), and the  $(x, y)$  plane represents our map of the universe. The inverse function  $W = \exp(Z/i)$  is the inverse map that takes a point in our map plane  $(x, y)$  back to the point it represents in the universe  $(u, v)$ . In the universe it is useful to establish polar coordinates  $(r, \theta)$  where

$$u = r \cos \theta \quad (16)$$

$$v = r \sin \theta \quad (17)$$

and  $r = (u^2 + v^2)^{1/2}$  is the (co-moving) distance from the center of the Earth and  $\theta = \arctan(v/u)$  is the right ascension measured in radians. Since

$$\cos \theta = \frac{e^{i\theta} + e^{-i\theta}}{2}, \quad \sin \theta = \frac{e^{i\theta} - e^{-i\theta}}{2i} \quad (18)$$

it is clear that

$$W = u + iv = r(\cos \theta + i \sin \theta) = re^{i\theta} \quad (19)$$

$$Z = i \ln(W) = i(\ln r + i\theta) = -\theta + i \ln r = x + iy \quad (20)$$

so:

$$x = -\theta \quad (21)$$

$$y = \ln r \quad (22)$$

Thus, the entire  $(u, v)$  plane, except the origin  $(0, 0)$ , is mapped into an infinite vertical strip of horizontal width  $2\pi$ , i.e.

$$-2\pi < x \leq 0, \quad -\infty < y < \infty \quad (23)$$

(Figure 6 shows the complex plane  $u+iv$  mapped onto the  $x+iy$  plane by this map. One can take this map and make it into a slide rule for multiplying complex numbers. Photocopy the map on this page and cut it out. Tape the left hand edge to the right hand edge to make a paper cylinder. The  $\theta$  coordinate now measures longitude angle on that cylinder. Now photocopy the map onto a transparency, and cut it out, and again tape the left hand edge to the right hand edge to make a transparent cylinder. In cutting out the left and right hand sides of the map cheat a little, cut along the outside edges of the map borderlines so that the circumference of the transparency cylinder is just a tiny bit larger than the paper cylinder and so that it will fit snugly over it. With the paper cylinder snugly inside the transparent cylinder you are ready to multiply. If you want to multiply two numbers  $A = a + bi$  and  $C = c + di$  all you do is rotate and slide the transparent cylinder until the transparency

number 1 (i.e.  $1 + 0i$ ) is directly over the number  $a + bi$  on the paper cylinder, then look up the number  $c + di$  on the transparent cylinder, below it on the paper cylinder will be the product  $A \cdot B$ . The logarithm of  $AB$  is equal to the sum of the logarithms of  $A$  and  $B$ . Of course, on the real axis,  $\theta = 0$  ( $x = 0$ ), the map looks like the scale on a slide rule. Alternatively make a flat slide rule for multiplying complex numbers: make two photocopies of the map on white paper and tape them together to make two cycles in  $\theta$  from right to left. Then make one photocopy of the map onto a transparency. Lay the number 1 (on the transparency) on top of the number  $A$  in the right hand cycle of the paper map and look on the transparency for the number  $B$ , below it on the paper map will be the product  $AB$ .)

For convenience on our map of the universe, let  $r = (\chi R_{H_0})/r_E$  (co-moving cosmological distance/radius of the Earth) be measured in units of the Earth's equatorial radius  $r_E = 6378\text{km}$ . Thus, circles of constant radius ( $r = \text{const.}$ ) from the center of the Earth are shown as horizontal lines ( $y = \text{const.}$ ) in the map, and rays of constant right ascension ( $\theta = \text{const.}$ ) are shown as vertical lines ( $x = \text{const.}$ ) in the map. The surface of the Earth (at its equator) is a circle of unit radius in the  $(u, v)$  plane, and is the line  $y = 0$  in the map. The region  $y < 0$  in the map represents the interior of the Earth, so one can show the Earth's mantle and liquid and solid core. The solid inner core has a radius about  $0.19 r_E$ , thus, the lower edge of the map must extend to  $y = \ln(0.19) = -1.66$  to show it. The region  $y > 0$  shows the universe beyond the Earth. The co-moving future observability limit at a radius of 19 Gpc is at  $9.2 \times 10^{19}$  Earth radii, and so the upper edge of the map must extend to  $y = \ln(9.2 \times 10^{19}) = 45.97$  to show it. Thus the dimensions of the map are  $\Delta x = 2\pi$ , and  $\Delta y = 47.63$ . The aspect ratio for the map is height/width = 7.58. See figure 7 for a small scale version of this that will fit on one page. (A square map would have dimensions  $2\pi \times 2\pi$  and would cover a scale ratio from bottom to top of  $\exp(2\pi) = 535.49$ . A map with an aspect ratio height/width = 7.58 covers a scale ratio from bottom to top of  $535.49^{7.58}$ .)

At a scale of about 1 radian per inch for the angular scale, this would make a map about 6.28 inches wide by 47.6 inches tall, which could be easily displayed as a wall chart. We have presented the map at approximately this scale later in this article.

This is not the first time logarithmic coordinates have been used for a map of the universe. The Amoco Map of Space Mysteries (De Peyng (1958)) plotted the curved surface of the Earth and above it altitude (from the surface, not distance from the center) marked off in equal intervals labeled 1 mile, 10 miles, 100 miles, 1,000 miles, 10,000 miles, 100,000 miles, 1 million miles, 10 million miles, and 100 million miles. In this range Solar system objects from the moon to Venus, Mars and the Sun are plotted properly. But although  $\alpha$  Centauri, the Milky Way and M31 are shown beyond they are not shown at correct scale (even logarithmically). The Earth's surface is plotted where an altitude of 0.1 miles should

have been. In any case, because of the curvature of the Earth’s surface in the map, even in the range between an altitude of 10 miles and 100 million miles, the map is not conformal. In October 1999, National Geographic presented a map of the universe (that one of us (JRG) participated in producing) which was a 3D view with a spherical Earth at the center with equal width shells surrounding it like an onion with radii of 400,000 miles, 40 million miles, 4 billion miles, 4 trillion miles, 10 light years, 1,000 light years, 100,000 light years, 10 million light years, 1 billion light years, 11-15 billion light years (Sloan et al. (1999)). This map displays objects from the moon to the microwave background but is also not conformal.

The map projection we are proposing is conformal because the derivatives of the complex function  $Z = i \ln W$  have no poles or zeros in the mapped region. If we want to see how a little area of the universe slice is mapped onto our slice we should do a Taylor expansion: the point  $W + \Delta W$  is mapped onto the point  $Z + \Delta Z = Z + (dZ/dW)\Delta W$  in the limit where  $\Delta W \rightarrow 0$  providing that  $dZ/dW \neq \infty$  so the map doesn’t blow up there and  $dZ/dW \neq 0$  so that the second and higher order terms in the Taylor expansion can be ignored (providing that none of the higher derivatives  $d^n Z/dW^n$  become infinite at the point  $W$ ). In this case, in the limit as  $\Delta W \rightarrow 0$ , the Taylor series is valid using just the first derivative term:

$$\Delta Z = \frac{dZ}{dW} \Delta W \quad (24)$$

$$\frac{dZ}{dW} = \frac{d(i \ln W)}{dW} = \frac{i}{W} \quad (25)$$

Thus for  $W \neq 0$  and finite (i.e. excluding the center of the Earth and the point at infinity which are not mapped anyway)  $dZ/dW$  is neither zero nor infinity. The higher derivatives ( $n \geq 2$ ) :  $d^n Z/dW^n = i(-1)^n n! W^{-n+1}$  are also finite when  $W$  is finite and non zero. Thus, the point  $W + \Delta W$  is mapped onto the point  $Z + \Delta Z = Z + dZ/dW \Delta W$  in the limit where  $\Delta W \rightarrow 0$ . Characterize the point  $W$  as

$$W = r_w(\cos \theta_w + i \sin \theta_w) \quad (26)$$

Now the product of two complex numbers

$$\begin{aligned} A &= r_a(\cos \theta_a + i \sin \theta_a) \\ B &= r_b(\cos \theta_b + i \sin \theta_b) \end{aligned}$$

is

$$A \cdot B = r_a r_b (\cos(\theta_a + \theta_b) + i \sin(\theta_a + \theta_b)), \quad (27)$$

so

$$\frac{1}{W} = \frac{1}{r_w} (\cos(-\theta_w) + i \sin(-\theta_w)), \quad (28)$$

and since  $i = \cos(\pi/2) + i \sin(\pi/2)$ ,

$$i \frac{1}{W} = \frac{1}{r_w} (\cos(\frac{\pi}{2} - \theta_w) + i \sin(\frac{\pi}{2} - \theta_w)) \quad (29)$$

and

$$\begin{aligned} \Delta Z &= r_{\Delta Z} (\cos \theta_{\Delta Z} + i \sin \theta_{\Delta Z}) \\ &= \frac{1}{r_w} (\cos(\frac{\pi}{2} - \theta_w) + i \sin(\frac{\pi}{2} - \theta_w)) \cdot r_{\Delta W} (\cos \theta_{\Delta W} + i \sin \theta_{\Delta W}) \\ &= \frac{r_{\Delta W}}{r_w} (\cos(\theta_{\Delta W} + \frac{\pi}{2} - \theta_w) + i \sin(\theta_{\Delta W} + \frac{\pi}{2} - \theta_w)) \end{aligned} \quad (30)$$

Thus, the vector  $\Delta W$  is rotated by an angle  $\pi/2 - \theta_w$  and multiplied by a scale factor of  $1/r_w$ . Since any two vectors  $\Delta W_1$  and  $\Delta W_2$  at the point  $W$  will be rotated by the same amount when they are put on the map the angle between them is preserved in the map, and so the map projection is conformal. The only place the first derivative (and the higher derivatives) blow up (or go to zero) is at  $W = 0$  at the center of the Earth or at the point at infinity  $W = \infty$ . But the Earth's center does not appear on the map at all (it is at  $y = -\infty$ ). This is a set of measure zero. Likewise, the point at infinity  $W = \infty$  is not plotted either (it is at  $y = +\infty$ ). So the map projection is conformal at all points in the map. Shapes are preserved locally.

The conformal map projection for showing the universe presented here was developed by JRG in 1972, and he has produced various small versions of it over the years. These have been shown at various times, notably to the visiting committee of the Hayden Planetarium in 1996 and to the staff of the National Geographic Society in 1999. Recent discoveries within a wide range of scales from the solar system objects, to the SDSS galaxies and quasars have prompted us to produce and publish the map in a large scale format.

Our large scale map is shown in figure 8 (the foldout). A radial vector  $\Delta W$  (pointing away from the Earth's center) at the point  $W$  points in the direction  $\theta_{\Delta W} = \theta_w$ . This vector in the map is rotated by an angle  $\pi/2 - \theta_w$  so that  $\theta_{\Delta Z} = \theta_{\Delta W} + \pi/2 - \theta_w = \pi/2$ , so that it points in the vertical direction. Small regions in the universe are rotated in the map so that the radial direction, away from the center of the Earth, is in the vertical direction in the map. Radial lines from the Earth's center are plotted as vertical lines. Circles of constant radius from the center of the Earth are horizontal lines. The length of the vector  $\Delta W$  is multiplied by a scale factor  $1/r_w$ . Thus, the scale factor at a given point on the map can be read off as proportional to 1 over the distance of the point from the Earth,  $r_w$ . (Objects that are twice as far away are shown at 1/2 scale and objects that are 10 times further away are shown at 1/10th the scale, and so forth).

Radial lines separated by an angle  $\theta$  (in radians), going outward from the Earth will be plotted as parallel vertical lines separated by a horizontal distance proportional to  $\theta$ . Thus objects of the same angular size in the sky (as seen from the center of the Earth) will be plotted as the same size on the map. The Sun and Moon which have the same angular size in the sky ( $0.5^\circ$ ) will be plotted as circles of the same size on the map (since their cross sections are circles and shapes are preserved locally in a conformal map projection).

The map gives us that Earthling's view of the universe that we want. Objects are shown at a size in the map proportional to the size they subtend in the sky. The Sun and Moon are equally large in the sky and so appear of the same size in the map. Objects that are close to us are more important to us – as depicted in that New Yorker cover. Buildings on 9<sup>th</sup> avenue may subtend as large an angle to our eye as the distant state of California. Our loved ones – important to us – are often only a few feet away and subtend a large angular scale to our eyes. A murder occurring in our neighborhood draws more of our attention than a murder of someone halfway around the globe. Plotting objects at a size equal to their angular scale makes psychological sense. Objects are shown taking up an area on the map that is proportional to the area they subtend in the sky (if they are approximately spherical – as many astronomical bodies are). The importance of the object in the map (the fraction of the map it takes up) is proportional to the chance we will see the object if we look out along a random line of sight. Indeed, if we look at the map from a constant distance, the angular size of the objects in the map will be proportional to the angular size they subtend in the sky. The visual prominence of objects in the map will be proportional to their visual prominence in the sky.

Of course this means that the Moon and Sun and other objects will be shown at their true scale relative to their surroundings (i.e. the Moon is shown in correct scale relative to the circumference of its orbit) which is small because they are small in the sky. Suppose we made an Mollweide equal area map projection of the sky at a scale to fit on a journal page: an ellipse with horizontal width 6.28 inches and vertical height of 3.14 inches. Along the equatorial plane the scale is linear at 1 inch per radian. The diameter of the Moon or Sun is  $1/2^\circ$ , or  $1/720$ th of the  $360^\circ$  length around the equator. Thus, on this sky map the Moon would have a diameter of  $(6.28 \text{ inches})/720 = 0.0087 \text{ inches}$ . On our map the Moon would have a similar diameter, for the scale of our map is approximately 1 radian = 1 inch. The Moon and Sun are rather small in the sky. With a printer resolution of 300 dots per inch the Sun and Moon would then be approximately 3 dots in diameter. For easier visibility we have plotted the Sun and Moon as circles enlarged by a factor of 18. Similar enlargements of individual objects like the Sun and the Moon might appear on sky maps appearing on one page. Just as symbols for cities on world maps may be larger than the cities themselves. Still it is interesting to note what the true sizes on the map should be since it shows how much

empty space in the universe there is. M31 for example subtends an angle of about  $2^\circ$  on the sky and so would be about 0.035 inches on a map with 1 inch/radian scale. If versions of the map were produced at larger scale as we shall discuss below, images of the Sun, Moon, and nearby galaxies could be displayed at proper angular scale and simply placed on the map.

The completed map is shown in the foldout (figure 8).

The map shows a complete sample of objects in the classes we are illustrating in the equatorial slice ( $-2^\circ < \delta < 2^\circ$ ) which is shown conformally correct. These objects are shown at the correct distances and right ascensions. This we supplement with additional famous objects out of the plane which are shown at their correct distances and right ascensions. So this is basically an equatorial slice with supplements.

At the bottom, the map starts with an equatorial interior cross section of the Earth. First we see the solid inner core of the Earth with a radius of  $\sim 1200$  km. Above this is the liquid outer core (1200 km – 3480 km), and above that are the lower (3480 km – 5701 km) and upper mantle (5701 km – 6341 km). The Earth’s surface has an equatorial radius of 6378 km. There is a line designated Earth’s surface (& crust) which is a little thicker than an ordinary line to properly indicate the thickness of the crust. The Earth’s surface (& crust) line is shown as perfectly straight, because on this scale the altitude variation in the Earth’s surface is too small to be visible. The scale at the Earth surface line is approximately 1/250,000,000. The maximum thickness of the crust (37 km) is just barely visible on the map at a resolution of 300 dots per inch, so we have shown the maximum crust depth accordingly, by the width of the Earth surface (crust) line.

(If we had wished we could have extended the map downward to cover the entire inner solid core of the Earth down to the central neutron (or proton) in an iron atom located at the center of the Earth. Since a neutron has a radius of approximately  $1.2 \times 10^{-13}$  cm or  $1.9 \times 10^{-22} r_E$ , the circumference of this central neutron would be plotted as a straight line at  $y = -50.0$ . The outer circumference of the central iron atom (atomic radius of  $1.40 \times 10^{-8}$  cm, Slater (1964)) would be plotted as a straight line at  $y = -38.36$ . Thus, including the entire inner solid core of the Earth down to the central neutron in an iron atom at the center of the Earth would require (at 1 inch/radian scale) about an additional 48 inches of map, approximately doubling its length. The central atom and its nucleus would then occupy the bottom 11.6 inches of the map, giving a nice illustration of both the nucleus and all the electron orbitals. But since we are primarily interested in astronomy, and the key regions of the Earth’s interior are covered in the map already, we have stopped the map just deep enough to show the extent of the inner solid core.)

We have shown the Earth’s atmosphere above the Earth’s surface. The ionosphere

is shown which occupies an altitude range of 70 – 600 km. Below the ionosphere is the stratosphere which occupies an altitude range of 12 – 50 km. Although there was not enough space to include a label, the stratosphere on the map simply occupies the tiny space between the lower error bar indicating the bottom of the ionosphere and the "surface of the Earth" line. The troposphere (0 – 12 km) is of such small altitude that it is subsumed into the Earth's surface line thickness. Above the ionosphere we have formally the exosphere, where the mean free path is sufficiently long that individual atoms with escape velocity can actually escape. So the top of the ionosphere effectively defines the outer extent of the Earth's atmosphere and the map shows properly just how narrow the Earth's atmosphere is relative to the circumference of the Earth.

Next we have shown all 8,420 artificial Earth satellites in orbit as of Aug 12, 2003 (at the time of full Moon 2003/08/12 04:48 UT). In fact all objects in the map are shown as of that time. This is the last full Moon before the closest approach of Mars to the Earth in 2003. The time was chosen for its placement of the Sun, Moon and Mars. We show all Earth satellites (not just those 624 in the equatorial slice). These are actual named satellites, not just space junk. Some famous satellites are designated by name. ISS is the International Space Station. HST is the Hubble Space Telescope. These are both in low Earth orbit.

Vanguard 1 is shown, the earliest launched satellite still in orbit. The Chandra X-ray observatory is also shown. There are two main altitude layers of low Earth orbiting satellites and a scattering of them above that. There is a quite visible line of geostationary satellites at an altitude of 22,000 miles above the Earth's surface. These geosynchronous satellites are nearly all in our equatorial slice. A surprise was the line of GPS (Global Positioning System) satellites at a somewhat lower altitude. These are all in nearly circular orbits at identical altitudes and so also show up as a line on the map. We had not realized that there were so many of these satellites or that they would show up on the map so prominently. The inner and outer Van Allen radiation belts are also shown.

Beyond the artificial Earth satellites and the Van Allen radiation belts lies the Moon, marking the extent of direct human occupation of the universe. The Moon is full on August 12, 2003.

Behind the full Moon at approximately 4 times the distance from Earth is the WMAP satellite which has recently measured the cosmic microwave background. It is in a looping orbit about the L2 unstable Lagrange point on the opposite side of the Sun from the Earth. Therefore it is approximately behind the full Moon.  $180^\circ$  away, at the L1 Langrange point is the Solar and Heliospheric Observatory (SOHO) satellite. From L1, SOHO has an unobstructed and uninterrupted view of the Sun throughout the year.

To illustrate the distances from Earth to the nearest asteroids, we plot the 12 closest to Earth as of August 12, 2003 (labeled NEOs - Near Earth Objects). Asteroid 2003 GY was closest to Earth at that time. Another two them are particularly interesting. Asteroid 2003 YN107 is currently the only known quasi-satellite of the Earth (Connors (2004)), and shall remain such until the year 2006. Asteroid 2002 AA29 is on an interesting horseshoe orbit (Connors (2002), Belbruno & Gott (2004)) that circulates at 1 AU and has close approaches to Earth every 95 years. Such horseshoe orbits are typical of orbits that have escaped from the Trojan L4, L5 points (Belbruno & Gott (2004)). Since this asteroid may have originated at 1 AU like the Earth and the great impactor that formed the Moon, it might be an interesting object for a sample return mission, as Gott and Belbruno have noted.

Mars is shown at approximately 9,000 Earth radii, or 0.4 astronomical units (as seen on the scale on the right). Mars is near its point of closest approach (which it achieved on August 27, 2003 when it was at a center-to-center distance of 55,758,006 km). Further up are Mercury, the Sun and Venus. Venus is near conjunction with the Sun on the opposite side of its orbit. The Sun is  $180^\circ$  away from the Moon or halfway across the map horizontally, since the Moon is full. The Sun is 1 AU away from the Earth. At distances from Earth of between  $\sim 0.7$  to  $\sim 5$  AU are the main belt asteroids. Here, out of the total of 218,484 asteroids in the ASTORB database, we have shown only those 14,183 which are in the equatorial plane equatorial slice ( $-2^\circ < \delta < 2^\circ$ ). If we had shown them all, it would have been totally black. By just showing the asteroids in the equatorial slice we are able to see individual dots. In addition, some famous main belt asteroids, like Ceres, Eros, Gaspra, Vesta, Juno and Pallas are shown (even if off the equatorial slice) and indicated by name. The width of the main belt of asteroids is shown in proper scale relative to its circumference in the map. The belt is closer to the Earth in the anti-solar direction since it is an annulus centered on the Sun and the Earth is off center. Because the main belt asteroids lie approximately in the ecliptic plane which is tilted at an angle of  $23.5^\circ$  relative to the Earth's equatorial plane, there are two dense clusters where the ecliptic plane cuts the Earth's equatorial plane and the density of asteroids is highest. One intersection is at about 12h and the other is at 24h.

Jupiter is shown in conjunction with the Sun approximately 6 AU from the Earth. On either side of Jupiter we can see the two swarms of Trojan asteroids trapped in the L4 and L5 stable Lagrange equilibrium points  $\pm 60^\circ$  away from Jupiter along its orbit. From the vantage point of Earth, 1 AU off center opposite Jupiter in its orbit, the Trojans are a bit closer to the Earth than Jupiter and a bit closer to Jupiter in the sky on each side than  $60^\circ$ . The Ulysses spacecraft is visible near Jupiter. It is in an orbit far out of the Earth's equatorial plane, but we have included it anyway. Beyond Jupiter are Saturn, Uranus and Neptune.

Halley’s comet is shown between the orbits of Uranus and Neptune, as of August 12, 2003.

Next we show Pluto and the Kuiper belt objects. We are showing all 772 of the known Kuiper belt objects (rather than just those in the equatorial plane). It is surprising how many of them there are. Recently discovered 2003 VB12 (“Sedna”), Quaoar and Varuna, the largest KBOs currently known, are also shown and labeled. Sedna is currently the second largest known transneptunian object, after Pluto (Brown, Trujillo, & Rabinowitz (2004)). The band of Kuiper belt objects is relatively narrow because of the selection effect that objects of a given size become dimmer approximately as the fourth power of their distance from the Earth and Sun. The band of Kuiper belt objects has vertical density stripes, again due to angular selection effects depending on where various surveys were conducted. A sprinkling of Kuiper belt objects extend all the way into the space between the orbit of Uranus and Saturn (the “Centaurs”, of which we’re only plotting the ones in the equatorial plane).

We show Pioneer 10, Voyager 1 and Voyager 2 spacecrafts, headed away from the solar system. These are on their way to the heliopause, where the solar wind meets the interstellar medium. They have not reached it yet.

Almost a hundred times further away than the heliopause is the beginning of the Oort cloud of comets which extends from about 8,000 AU to 100,000 AU. A comet entering the inner solar system for the first time has a typical aphelion in this range.

Beyond the Oort Cloud are the stars. The ten brightest stars visible in the sky are shown with large star symbols. The nearest star, Proxima Centauri is shown with a small star symbol. Proxima Centauri, an M5 star, is a member of the  $\alpha$  Centauri triple star system.  $\alpha$  Centauri A, at a distance of a little over 1 pc (see scale on the left), and a solar type star, is one of the ten brightest stars in the sky. The 10 nearest star systems are also shown:  $\alpha$  Centauri, Barnard’s star, Wolf 359, Halande 21185, Sirius, UV and BL Ceti, Ross 154, Ross 248,  $\epsilon$  Eridani and Lacaille 9352. Of these,  $\epsilon$  Eridani has a confirmed planet circling it.

Stars with known confirmed planets circling them (with  $M \sin i < 10M_{\text{Jupiter}}$ ) are shown as dots with circles around them. Of these, 95 are solar type stars whose planets were discovered by radial velocity perturbations. Some of the more famous ones like 51 Peg, 70 Vir, and  $\epsilon$  Eri are labeled. The star HD 209458 has a Jupiter-mass planet which was discovered by radial velocity perturbations but was later also observed in transit (Mazeh et al. (2000), Henry et al. (1999)). The first planet discovered by transit was OGLE-TR-56 which lies at a distance of over 1 kpc from the Earth. Three other OGLE stars were also found to have transiting planets – TR-111, TR-113 and TR-132. These were all in the same field (R.A.  $\sim 10^{\text{h}}50^{\text{m}}$ ) at approximately the same distance ( $\sim 1.5\text{kpc}$ ) and so would

be plotted at positions on the map that would be indistinguishable. The planet TrES-1 around GSC 02652-01324 was recently discovered by transit and confirmed by radio velocity measurements (Alonso et al. (2004)). A planet circling the star OGLE 2003-BLG-235 was discovered by microlensing (Bond et al. (2004)). PSR 1257+12 is a pulsar (neutron star) with three terrestrial planets circling it which were discovered by radial velocity perturbations on the pulsar revealed by accurate pulse timing (Wolszczan & Frail (1992), Wolszczan (1994)). This was the first star discovered to have planets. Also, SO 0253+1652 is shown and labeled on the map. It is the closest known brown dwarf (Teegarden (2003)), at 3.82pc.

The first radio transmission of any significant power to escape beyond the ionosphere was the TV broadcast of the opening ceremony of the 1936 Berlin Olympics on August 1<sup>st</sup>, 1936, a fact noted by Carl Sagan in his book Contact. The wave front corresponding to this transmission is a circle having a radius of  $\sim 10^{11}$  Earth radii on August 12, 2004, and is indicated by the straight line labeled "Radio signals from Earth have reached this far". Radio signals from Earth have passed stars below this line.

The Hipparcos satellite has measured accurate parallax distances to 118,218 stars (ESA (1997)). We show only the 3,386 Hipparcos stars in the equatorial plane ( $-2^\circ < \delta < 2^\circ$ ).

Other interesting representative objects in the galaxy are illustrated: the Pleiades, the globular cluster M13, the Crab nebula (M1), the black hole Cygnus X-1, the Orion Nebula (M42), the Dumbbell nebula and the Ring nebula, the Eagle nebula, the Vela pulsar, and the Hulse-Taylor binary pulsar. At a distance of 8 kpc is the Galactic Center which harbors a 2.6 million solar mass black hole. The outermost extent of the Milky Way optical disk is shown as a dotted line.

Beyond the Milky Way are plotted 52 currently known members of the Local Group of galaxies. We have included all of these, not just the ones in the equatorial plane. These are indicated by dots or triangles. M31's companions M32 and NGC205 are shown as dots but not labeled since they are so close to M31.

M81, is the first galaxy shown beyond the Local Group and is a member of the M81 – M82 group. Its distance was determined by Cepheid variables using the HST. Other famous galaxies labeled include M101, the Whirlpool galaxy (M51), the Sombrero galaxy, and M87, in the center of the Virgo cluster. If we showed all the M objects many would crowd together in a jumble at the location of the Virgo cluster. M87 harbors in its center the largest black hole yet discovered with a mass of  $3 \times 10^9$  solar masses.

The dots appearing beyond M81 in the map are the 126,594 SDSS galaxies and quasars (with  $z < 5$ ) in the equatorial plane equatorial slice ( $-2^\circ < \delta < 2^\circ$ ). In addition, all 31 currently known SDSS quasars with  $z > 5$  are plotted, not just those in the equatorial slice.

Since these large redshift quasars are shown from all over the sky, a number of them appear at right ascensions which occur in the zone of avoidance for the equatorial slice. The upper part of our map can be compared directly with figure 1 and figure 2. The map shows clearly and with recognizable shape all the structures shown in the close-up in figure 2, while still showing all the SDSS quasars shown in the full view in figure 1. The logarithmic scale captures both scales beautifully. On the left, (at about 1.5h and 120 Mpc) we can see clearly the large circular void visible in figure 2. To the right, at RA of 9h-14h and at a distance of 215 – 370 Mpc we can see a Sloan Great Wall in the SDSS data, longer than the Great Wall of Geller and Huchra (the CfA2 Great Wall). The blank regions are where the Earth’s equator cuts the galactic plane and intersects the zone of avoidance near the galactic plane (where the interstellar dust obscures distant galaxies and which the Sloan survey does not cover). These are empty fan-shaped regions as shown in figure 1 and figure 2, bounded by radial lines pointing away from the Earth, so on our map these are bounded by vertical straight lines.

The Great Attractor (which is far off the equatorial plane and toward which the Virgo super cluster has a measurable peculiar velocity) is shown.

The most prominent feature of the SDSS large scale structure seen in figure 8 is the “Sloan Great Wall”. This feature was noticed early-on in the Sloan data acquisition process, and has been mentioned in passing in a couple of times in Sloan reports, accompanied by phrases such as “large” (Blanton et al. (2003)), and “striking”, “wall-like”, and “may be the largest coherent structure yet observed” (Tegmark et al., astro-ph/0310725). To make a quantitative comparison, we have also shown the Great Wall of Geller and Huchra. This extends over several slices of the CfA2 survey (from  $42^\circ$  to  $-8.5^\circ$  declination). Rather than plotting points for it here, which would be confused with SDSS survey galaxies we have plotted density contours averaging over all the CfA2 slices from  $42^\circ$  to  $-8.5^\circ$  declination. This volume extends far above the equatorial plane, and since we are plotting it in right ascension correctly, it is not presented conformally, but is being lengthened in the tangential direction by a factor of  $\sim 1/\cos(21^\circ) = 1.07$ . Note that since the CfA2 Great Wall is a factor of approximately 2.5 closer to us than the Sloan Great Wall it is depicted at scale that is 2.5 times larger. So although the CfA2 Great Wall stretches from 9h to 16.7h (or 7.7 hours of right ascension), as compared with the SDSS Great Wall which stretches from 8.7h to 13.7h (or 5 hours of right ascension) its real length in co-moving coordinates relative to the CfA2 Great Wall is, by this simple analysis,  $2.5 \times 5 / (7.7 \times 1.07) \approx 1.74$  times as long. This is apparent in the comparison figure supplied in figure 9, where both are shown at the same scale in co-moving coordinates. To make a fair comparison, since the Great Wall is almost a factor of 3 closer than the Sloan Great Wall, we have plotted a  $12^\circ$  wide slice from the CfA2 survey to compare with our  $4^\circ$  wide slice in the Sloan, so that both slices have

approximately the same width at each wall.

Of course, the walls are not perfectly aligned with the  $x$  axis of our map, so one has to measure their length along the curve. The Sloan Great Wall is at a median distance of 310 Mpc. It's total length in co-moving coordinates is 450 Mpc as compared with the total length of the Great Wall of Geller and Huchra which is 240 Mpc long in co-moving coordinates. This indicates the sizes the two walls would have at the current epoch. But the Great Wall is at a median redshift of  $z = 0.029$  so it's true size at the epoch we are observing it is smaller by a factor of  $1 + z$  giving it an observed length of 232.64 Mpc (or 758 million light years). The Sloan great wall is at a redshift of  $z = 0.073$  so it's true observed length is 419 Mpc (or 1,365 million light years). For comparison, the CMB sphere has an observed diameter of  $(2 \cdot 14,000)/1090 = 25.7$  Mpc. The observed length of the Sloan Great Wall is thus 80% greater than the Great Wall of Geller and Huchra.

Since we have numerous studies that show that the 3D topology of large scale structure is spongelike (Gott, Dickinson, & Melott (1986); Vogeley et al. (1994); Hikage et al. (2002)) it should not be surprising that as we look at larger samples we should find examples of larger connected structures. Indeed, we would have had to have been especially lucky to have discovered the largest structure in the observable universe in the initial CfA survey which has a much smaller volume than the Sloan survey. Simulated slices of the Sloan using flat lambda models (as suggested by WMAP) show great walls and great wall complexes that are quite impressive (Colley et al. (2000)). Cole, Hatton, Weinberg, & Frenk (1998) for example had a great wall in their  $\Omega_m = 0.4$ ,  $\Omega_\Lambda = 0.6$  Sloan simulation which is 8% longer than the Great Wall of Geller and Huchra; and so it could be said that the existence of a Great Wall in the Sloan longer than the Great Wall of Geller and Huchra was predicted in advance. Visual inspection of the 275 PThalos simulations reveals similar structures to the Sloan Great Wall in more than 10% of the cases (Tegmark et al, astro-ph/0310725). Thus, it seems reasonable that the Sloan Great Wall can be produced from random phase Gaussian fluctuations in a standard flat-lambda model, a model that also predicts a spongelike topology of high density regions in 3D. Notably, our quantitative topology algorithm applied to the 2D Sloan Slice identifies the Sloan Great Wall as one connected structure (Hoyle et al. (2002)). Figure 2 in Hoyle et al. (2002) clearly shows this as one connected structure at the median density contour when smoothed at  $5h^{-1}$  Mpc in a volume limited sample where the varying thickness and varying completeness of the survey in different directions are accounted for. It is perhaps no accident that both the Sloan Great Wall and the Great Wall of Geller and Huchra are seen roughly tangential to the line of sight. Great Walls tangential to the line of sight are simply easier to see in slice surveys, as pointed out by Praton, Melott, & McKee (1997). A Great Wall perpendicular to the line of sight would be more difficult to see because the near end would be lost due to thinness of the slice and the far end would be lost due to the

lack of galaxies bright enough to be visible at great distances. Redshift space distortions on large scales, i.e. infall of galaxies from voids onto denser regions enhances contrast for real features tangential to the line of sight. "Fingers of God" also make tangential structures more noticeable by thickening them. When Park (1990) first simulated a volume large enough to simulate the CfA survey, a Great Wall was immediately seen in the 3D data. When a slice to simulate the CfA slice seen from Earth – which gets wider as it gets further from the Earth – was made, the Great Wall in the simulation was pretty much a dead ringer for the Great Wall of Geller and Huchra – equal in length, shape, and density. This was an impressive success for N-body simulations. The Sloan Great Wall and the CfA Great Wall have been found in quite similar circumstances, each in a slice of comparable thickness, and as illustrated in figure 9, both are qualitatively quite similar except that the Sloan Great Wall is simply larger, and as we have noted, our 2D topology algorithm (Hoyle et al. (2002)) identifies the Sloan Great Wall as one connected structure in a volume limited survey where the varying thickness and completeness of the slice survey are properly accounted for. The CfA Great Wall is as large a structure as could have fit in the CfA sample, but the Sloan Great Wall is smaller than the size of the Sloan survey, showing the expected approach to homogeneity on the very largest scales.

The 2dF survey (Colless et al. (2001)), of similar depth to the Sloan, completed two slices, an equatorial slice ( $9^h : 50^m < \alpha < 14^h : 50^m, -7.5^\circ < \delta < 2.5^\circ$ ), and a southern slice ( $21^h : 40^m < \alpha < 03^h : 40^m, -37.5^\circ < \delta < -22.5^\circ$ ). This survey was thus not appropriate for our logarithmic map of the universe. The southern slice was not along a great circle in the sky, and therefore would be stretched if plotted in our map in right ascension. The equatorial slice was of less angular extent than the corresponding Sloan Slice and so the Sloan with its greater coverage in a flat equatorial slice was used to plot large scale structure in our map. Indeed, the 2dF survey, because of its smaller coverage in right ascension, missed the western end of the Sloan Great Wall and so the wall did not show up as prominently in the 2dF survey as in the Sloan. Power spectrum analysis of the 2dF and the Sloan come up with quite similar estimates. These two great surveys in many ways complement each other. Perhaps most importantly the 2dF power spectrum analysis which was available before Sloan and in time for WMAP allowed estimates of  $\Omega_m$  which allowed WMAP to refine the cosmological parameters used in the construction of this map. The Sloan Great Wall contains a number of Abell clusters (including, for example, A1238, A1650, A1692 and A1750 for which redshifts are known). The spongelike nature of 3D topology means that clusters are connected by filaments or walls but if extended far enough, walls should show holes allowing the voids on each side to communicate.

Indeed, in our map we can see some remnants of the CfA2 Great Wall (a couple of clumps or "legs") extending into the equatorial plane of the Sloan sample. As shown in

Vogeley et al. (1994), if extended to the south the Great Wall develops holes that allow the foreground and background voids to communicate leading to a spongelike topology of the median density contour surface in 3D. In 3D, the Sloan Great Wall may be connected to the supercluster of Abell clusters found by Bahcall and Soneira (Bahcall & Soneira (1984)) whose two members lie just above it in declination.

In the center of the Great Wall is the Coma Cluster, one of the largest clusters of galaxies known.

The quasar 3C273 is shown as a cross.

The gravitational lens quasar 0957 is shown as well as the lensing galaxy producing the multiple image. The lensing galaxy is along the same line of sight but at about one third the co-moving distance.

The gamma ray burster GRB990123 is shown - for a brief period this was the most luminous object in the observed universe.

The redshift  $z = 0.76$  is shown as a line which marks the epoch that divides the universe's decelerating and accelerating phase. Objects closer than this line are observed at an epoch when the universe's expansion is accelerating, while objects further away than this line are observed at an epoch when the universe's expansion is decelerating.

The unreachable limit is shown at  $z = 1.69$ . Because of the acceleration of the expansion of the universe, photons sent from Earth now will never reach objects beyond this line. Galaxies beyond this line will never hear our current TV signals. Spaceships from Earth, traveling slower than light will also find the territory beyond this line unreachable. This redshift is surprisingly low. It is interesting that we can see many objects today that are so far away that we can never get to them.

SDSS quasars in the equatorial plane ( $-2^\circ < \delta < 2^\circ$ ) are shown as points out to a redshift of  $z = 5.0$  using redshifts determined from the SDSS survey spectra. For quasars with  $z > 5.0$  we have shown all 31 quasars from the SDSS with  $z > 5$  regardless of declination. There are now a surprisingly large number of quasars with  $z > 5$  known. Because a number of these are at high declination, they occur at right ascensions that are in the zone of avoidance for the equatorial plane. Each is shown at its proper right ascension and distance, including the largest redshift one with  $z = 6.42$  which is labeled (M. Strauss 2003, private communication). This is currently the largest redshift quasar known.

The galaxy SDF J132418.3+271455 with the largest accurately measured redshift ( $z = 6.578$ ) is also shown. This was discovered in the Subaru Deep Field (Kodaira et al. (2003)).

The co-moving distance at which the first stars are expected to form is shown as a dashed line. The WMAP satellite has found that the first stars appear about 200 million years after the Big Bang and the map therefore indicates the distance out to which stars could be seen in principle.

Finally there is the cosmic microwave background radiation discovered by Penzias and Wilson in 1965 (Penzias & Wilson (1965)). CMB photons from this surface arrive directly from an epoch only 380,000 years after the Big Bang.

A line showing the co-moving radius back to the Big Bang is also shown. This represents seeing back to the epoch just after inflation. The co-moving distance between the cosmic microwave background and the Big Bang is shown in correct proportion to the circumference. In comparing with figure 1, we note that in that map the circumference is a factor of  $\pi$  larger. So in our map, which shows the  $360^\circ$  circumference of the cosmic microwave background as approximately the same length as the diameter of the circle in figure 1, the scale at that point is about a factor of  $\pi$  smaller than in figure 1 and the cosmic microwave background and the Big Bang are closer to each other (by a factor of  $\pi$ ) than in figure 1 as expected.

Last is shown the co-moving future visibility limit. If we wait until the infinite future we will eventually be able to see the Big Bang at the co-moving future visibility limit. Stars and galaxies that lie beyond this co-moving future visibility limit are forever hidden from our view. Because of the de Sitter expansion produced by the cosmological constant the universe has an event horizon which we cannot see over no matter how long we wait.

It is remarkable how many of the features shown in this map have been discovered in the current astronomical generation. When one of us (JRG) began studying astronomy at age 8 (in 1955), on astronomical maps there were no artificial satellites, no Kuiper belt objects, no other stars with planets, no brown dwarfs, no pulsars, no black holes, no non-solar X-ray sources, no gamma ray bursters, no great walls, no great attractors, no quasars, no gravitational lenses, and no observation of the cosmic microwave background.

#### 4. Applications

This map shows large scale structure well. "Fingers of God" are vertical which makes removing them for large scale structure purposes particularly easy. A test for roundness of voids as proposed by Ryden (1995) – the Alcock-Paczynski isotropy test – could be done on this map as well as on the co-moving map. The ability of this test to differentiate between cosmological models can be deduced by measuring void isotropy as a function of cosmological model in the plane of parameters ( $\Omega_m, \Omega_\Lambda$ ). For the correct cosmological model the void

pictures will be isotropic (since the Earth is not in a special position in the universe). To do this test we need conformal maps for various cosmological models, and so we need conformal maps for the  $k = +1$  and  $k = -1$  cases as well as the  $k = 0$  case so that statistical comparisons can be made. The formulas for these projections are given in the appendix.

A Fourier analysis of large scale structure modes in the map  $(k_x, k_y)$  can provide information on the parameter  $\beta = \Omega_m^{0.6}/b$  where  $b$  is the bias parameter. For fluctuations in the linear regime in redshift space  $d\rho/\rho \propto (1 + \beta\mu^2)$  where  $\mu = \cos\theta$  where  $\theta$  is the angle between the normal to the wave and the line of sight in 3D (Kaiser (1987)). Waves tangential to the line of sight have a larger amplitude in redshift space than waves parallel to the line of sight because the peculiar velocities induced by the wave enhance the amplitude of the wave when peculiar radial velocities are added to Hubble positions as occurs when galaxies are plotted using redshift at the Hubble flow positions assuming peculiar velocities are zero. Imagine a series of waves isotropic in 3D. Then one can show that the average value of  $\mu^2$  in 3D of those waves with an orientation  $\mu' = \cos(\phi)$  in the equatorial slice is  $\langle \mu^2 \rangle = (2/3)\mu'^2$ . Thus, we expect approximately, for waves observed in our equatorial slice  $\delta\rho/\rho \propto (1 + [2/3]\beta\mu'^2)$ . Waves in our map with constant  $(k_x, k_y)$  represent global logarithmic spiral modes with constant inclination relative to the line of sight. Of course this is an oversimplified treatment, since we must consider the power spectrum of fluctuations when relating the modes seen at a particular wavelength in the plane and in 3D and the "fingers of God" must be eliminated by some friend-of-friend algorithm. But in general, we expect that modes that are radial ( $k_x = 0$ ) will have higher amplitudes than modes that are tangential ( $k_y = 0$ ) and this effect can be used empirically, in conjunction with N-body simulations, to provide an independent check on the value of  $\beta$ . One simply adopts a cosmological model, checks with N-body simulations the relative amplitude of map modes as a function of  $\mu'$  in the logarithmic map and compares with the observations assuming the same cosmological model when plotting the logarithmic map: if the cosmological model  $(\Omega_m, \Omega_\Lambda)$  is correct, the results should be similar.

Since logarithmic spirals appear as straight lines in our map projection, it may prove useful for mapping spiral galaxies. Take a photograph of a face-on spiral galaxy, place the origin of the coordinate system in the center of the galaxy and then construct our logarithmic map of this 2D planar photograph. The spiral arms (which approximate logarithmic spirals) should then appear as straight lines on the conformal map. We have tried this on a face-on spiral galaxy photograph given to us by James Rhoads and the results were very satisfying. The spiral arms indeed were beautiful straight lines, and from their slope one could easily measure their inclination angle. Star images in the picture were still circular in the map because the map is conformal.

## 5. Conclusions

Maps can change the way we look at the world. Mercator’s map presented in 1569 was influential not only because it was a projection that showed the shapes of continents well but because for the first time we had pretty accurate contours for North America and South America to show. The Cosmic View and the Powers of Ten alerted people to the scales in the universe we had begun to understand. De Lapparent, Geller, and Huchra showed how a slice of the universe could give us an enlightening view of the universe in depth. Now that astronomers have arrived at a new understanding of the of the universe from the solar system to the cosmic microwave background, we hope our map will provide in some small way a new visual perspective on these exciting discoveries.

The map presented here is appropriate for use as a wall map. It’s scale is approximately 1 inch/radian. A version at twice the scale, 12.56 inches by 95.2 inches tall would also be appropriate for a wall chart and would run nearly from floor to ceiling in a normal room with an 8ft ceiling. If one wanted to show individual objects at  $60\times$  scale, the Moon and Sun would be 1 inch across, M31 would be 4 inches across, and Mars would be 0.0145 inches in diameter and Jupiter 0.0272 inches. Alternately the Sun and Moon and Messier objects could be shown a  $60\times$  scale with the planets at  $600\times$  scale to illustrate their usual appearance in small telescopes.

Consider some possible (and some fanciful) ways this map of the universe might be presented for educational use.

We have presented the map on the internet in color on astro-ph. In principle it would be easy to have such a map on the internet automatically continuously updated to track the current positions of the satellites, Moon, Sun, asteroids, planets, and Kuiper belt objects as a function of time, in fact we have plotted them as of a particular date and time using such programs. New objects could be added to the map as they were discovered. Click on an object, and a  $60\times$  enlarged view of it would appear. Two clicks, and a  $3600\times$  enlarged view would appear, and so forth – until the highest resolution picture available was presented. Individual images of all the SDSS galaxies and quasars shown on the map could be accessed in this way, as well as M objects . When an individual object was selected, helpful internet links to sites telling more about it would appear.

Since the left and right hand edges of the map are identical, the map could be profitably shown as a cylinder. In cylindrical form, the map at the approximate scale and detail of figure 7 is in perfect proportion to be used on a pencil with the Earth’s surface at the eraser end and the Big Bang at the point end. Perhaps the best cylindrical form for the map would be a cylinder on the interior of an elevator shaft for a glass elevator. Every floor you went up

you would be looking at objects that were 10 times further away than the preceding floor. A trip up such an elevator shaft could be simulated in a planetarium show, with the cylindrical map being projected onto the dome showing the view from the elevator as it rose.

We have put our map up on Princeton's flat video wall. This wall has a horizontal resolution of 4096 pixels. From top to bottom of the video wall is about 1600 pixels, so the scale change in the map from top to bottom is about a factor of 10. This shows a small portion of the entire map. We then scan this in real time moving steadily upward from the Earth to the cosmic microwave background and the Big Bang. This produces a virtual map 17.6 feet wide and 134 feet tall. With laser beams it would be easy to paint a large version of the map on the side of a building. A very large temporary version of our map of the universe could also be set up in a park or at a star party by simply planting markers for the salient objects.

The map could be produced on a carpet 6 feet wide 45.5 feet long for a hallway in an astronomy department or planetarium. Then every step you took down the hallway would take you about a factor of about ten further from the Earth – a nice way to have a walk through the Universe.

We would like to thank Michael Strauss for supplying us with the list of SDSS quasars with redshift greater than 5.

This work was supported by JRG's NSF grant AST04-06713.

Funding for the creation and distribution of the SDSS Archive has been provided by the Alfred P. Sloan Foundation, the Participating Institutions, the National Aeronautics and Space Administration, the National Science Foundation, the U.S. Department of Energy, the Japanese Monbukagakusho, and the Max Planck Society. The SDSS Web site is <http://www.sdss.org/>.

The SDSS is managed by the Astrophysical Research Consortium (ARC) for the Participating Institutions. The Participating Institutions are The University of Chicago, Fermilab, the Institute for Advanced Study, the Japan Participation Group, The Johns Hopkins University, the Korean Scientist Group, Los Alamos National Laboratory, the Max-Planck-Institute for Astronomy (MPIA), the Max-Planck-Institute for Astrophysics (MPA), New Mexico State University, University of Pittsburgh, Princeton University, the United States Naval Observatory, and the University of Washington.

### A. $k = +1, k = 0$ and $k = -1$ cases

Although the observations suggest the  $k = 0$  case is appropriate for the universe, for mathematical completeness we consider the general Friedmann metrics:

$$ds^2 = -dt^2 + a^2(t)[d\chi^2 + \sin^2 \chi(d\theta^2 + \sin^2 \theta \cdot d\phi^2)], \quad k = +1, \quad (\text{A1})$$

$$ds^2 = -dt^2 + a^2(t)[d\chi^2 + \chi^2(d\theta^2 + \sin^2 \theta \cdot d\phi^2)], \quad k = 0, \quad (\text{A2})$$

$$ds^2 = -dt^2 + a^2(t)[d\chi^2 + \sinh^2 \chi(d\theta^2 + \sin^2 \theta \cdot d\phi^2)], \quad k = -1 \quad (\text{A3})$$

Define the conformal time by:

$$\eta(t) = \int_0^t \frac{dt}{a} = \int_0^{a(t)} \left( -ka^2 + \frac{8\pi}{3}a^4\{\rho_m(a) + \rho_r(a)\} + \frac{\Lambda}{3}a^4 \right)^{-1/2} da \quad (\text{A4})$$

If we are currently at the epoch  $t_0$ , then the current conformal time is  $\eta(t_0)$ . When we look back to a redshift  $z$  we are seeing an epoch when  $a_0/a(t) = 1+z$ , and out to a co-moving distance  $\chi$  given by:

$$\chi(z) = \eta(t_0) - \eta(t) = \int_{\frac{a(t_0)}{1+z}}^{a(t_0)} \left( -ka^2 + \frac{8\pi}{3}a^4\{\rho_m(a) + \rho_r(a)\} + \frac{\Lambda}{3}a^4 \right)^{-1/2} da \quad (\text{A5})$$

As we have noted, in the flat case  $k = 0$ , we are free to adopt a scale for  $a$ , so we set  $a(t_0) = R_{H_0}$ .

For the  $k = +1$  case, a two dimensional slice through the universe is a sphere. So we need to make a conformal projection of the sphere onto a plane, and then we can apply our conformal logarithmic projection as before to produce our map. The stereographic map projection is such a conformal projection of a sphere onto a plane. Adopt coordinates on the sphere of  $\chi, \theta$ , where the metric on the sphere is given by:

$$ds^2 = a^2(t_0)(d\chi^2 + \sin^2 \chi \cdot d\theta^2) \quad (\text{A6})$$

Where the angle  $\theta$  is now a longitude (Thus,  $\theta$  is equivalent to  $\phi$  in metric A2 above – where in metric A2 we are considering the equatorial slice with  $\theta = \text{const.} = \pi/2$ . So to get the metric above from metric A2 we set  $\theta = \text{const.} = \pi/2$ , and replace  $\phi$  with  $\theta$ ). Now make a stereographic conformal projection of this sphere  $(\chi, \theta)$  onto a plane with polar coordinates  $(r, \theta)$ :

$$r = 2a(t_0) \tan\left(\frac{\chi}{2}\right) \quad (\text{A7})$$

$$\theta = \theta \quad (\text{A8})$$

This is a projection from the north pole onto a plane tangent to the south pole. The Earth would be at the south pole of the sphere (where  $\chi = 0$ ). A line from the north pole to the plane through the point  $(\chi, \theta)$  on the sphere will be at an angle  $\alpha = \chi/2$  relative to a normal to the plane, and also at an angle  $\alpha = \chi/2$  relative to a normal to the surface of the sphere at the point  $(\chi, \theta)$ , thus the foreshortening that occurs along the ray from the north pole as it crosses the surface of the sphere is exactly the same as the foreshortening that occurs when it crosses the surface of the plane. Thus, shapes in the surface are locally mapped without distortion locally onto the plane. The map is conformal. Now we have a conformal map of the sphere and we apply our logarithmic conformal map to the planar map to get our map of the universe:

$$x = -\theta \tag{A9}$$

$$y = \ln \frac{r}{r_E} = \ln \frac{2a(t_0) \tan(\frac{\chi}{2})}{r_E} \tag{A10}$$

This provides a conformal mapping from  $(\chi, \theta)$  to  $(x, y)$ . It is in fact a Mercator projection of the spherical section of the universe with the Earth located at the south pole of the sphere! We are used to seeing the Mercator projection for the surface of the Earth cut off at the Antarctic circle, so we do not see that if it were extended much nearer to the south pole (in the limit as  $\chi \rightarrow 0$ ) it would approximate our logarithmic map of a plane in the region of the south pole. (This projection would be useful for cosmological models that were slightly closed.)

For the  $k = -1$  case, a 2D slice of the universe is a negatively curved pseudosphere with metric:

$$ds^2 = a^2(t_0)(d\chi^2 + \sinh^2 \chi(d\theta^2)), \quad k = -1 \tag{A11}$$

Where  $\chi$  is the co-moving radius, and as before we have set  $\theta = \text{const.} = \pi/2$ , in metric A3 above to look at an equatorial slice, and we have replaced  $\phi$  in metric A3 with  $\theta$ , so that  $\theta$  is now a longitude. We can conformally project the pseudosphere onto plane with a map projection that is an analogue of the stereographic projection for the sphere. The metric above for a pseudosphere of radius  $a(t_0)$  is the metric on the hyperboloid surface:

$$x^2 + y^2 - t^2 = -a^2(t_0) \tag{A12}$$

where  $t > 0$  in a three dimensional Minkowski space with metric:

$$ds^2 = -dt^2 + dx^2 + dy^2 \tag{A13}$$

define coordinates on this surface  $(\chi, \theta)$  by

$$t = a(t_0) \cosh \chi \tag{A14}$$

$$y = a(t_0) \sinh \chi \sin \theta \tag{A15}$$

$$x = a(t_0) \sinh \chi \cos \theta \tag{A16}$$

with the definitions above it is easy to see that  $x^2 + y^2 - t^2 = -a^2(t_0)$ , since  $a^2(t_0) \sinh^2 \chi \cos^2 \theta + a^2(t_0) \sinh^2 \chi \sin^2 \theta - a^2(t_0) \cosh^2 \chi = -a^2(t_0)$ . Connect each point  $(\chi, \theta)$  on the surface with the origin  $(x, y, t) = (0, 0, 0)$  via a straight worldline. This worldline has a velocity relative to the  $t$  axis of  $v = \sinh \chi / \cosh \chi = \tanh \chi$ . So this worldline has a boost of  $\chi$  relative to the  $t$  axis. This worldline is normal to the surface at the point  $(\chi, \theta)$ , because that boost takes the  $t$  axis to the worldline in question and leaves the hyperbolic surface invariant. Let the intersection of that worldline with the tangent plane  $t = a(t_0)$  be the gnomonic map projection of the point  $(\chi, \theta)$  onto the plane with polar coordinates  $(r, \theta)$ . Then

$$r = a(t_0) \tanh \chi \quad (\text{A17})$$

$$\theta = \theta \quad (\text{A18})$$

This gnomonic projection maps the pseudosphere  $0 \leq \chi \leq \infty$  into a disk of radius  $r = a(t_0)$ . Why? Because in a time  $t = a(t_0)$  the worldline which has a velocity  $v = \tanh \chi$  travels a distance of  $r = vt = a(t_0) \tanh \chi$ . This gnomonic projection is not conformal, because the worldline is normal to the hyperboloid surface but not normal to the plane  $t = a(t_0)$ . This gnomonic projection maps geodesics on the negatively curved hyperboloid onto straight lines on the plane  $t = a(t_0)$  because any plane in the space  $(x, y, t)$  passing through the origin intersects the surface in a geodesic and this plane will intersect the tangent plane  $t = a(t_0)$  in a straight line.

A conformal projection, like the stereographic projection of the sphere is provided for the pseudosphere by connecting with a worldline each point on the surface  $(\chi, \theta)$ , to the point  $(x, y, t) = (0, 0, -a(t_0))$ , and letting this worldline intersect the plane  $t = a(t_0)$  at a point  $(r, \theta)$ . Now that worldline has a velocity  $v = \sinh \chi / (\cosh \chi + 1) = \tanh(\chi/2)$  (using a half angle trigonometric identity). Thus, this worldline has a boost relative to the  $t$  axis of  $\chi/2$  and therefore a boost of  $\chi/2$  relative to the normal to the plane  $t = a(t_0)$ . When it intersects the hyperbolic surface at the point  $(\chi, \theta)$ , the normal to the hyperbolic surface at that point has a boost of  $\chi$  relative to the  $t$  axis in the same plane. Thus, the worldline has a boost of  $\chi/2$  relative to the normal of the tangent plane and also a boost of  $\chi/2$  relative to the hyperbolic surface, so it has an equal boost (and observes equal Lorentz contractions) relative to both (giving identical foreshortenings as in the stereographic projection of the sphere) and therefore the map projection is conformal. This worldline connecting the point  $(x, y, t) = (0, 0, -a(t_0))$  to the point  $(\chi, \theta)$  on the surface thus intersects the tangent plane  $t = a(t_0)$  at the point  $(r, \theta)$  given by

$$r = 2a(t_0) \tanh\left(\frac{\chi}{2}\right) \quad (\text{A19})$$

$$\theta = \theta \quad (\text{A20})$$

This maps the pseudosphere  $0 \leq \chi < \infty$  into a disk of radius  $r = 2a(t_0)$ . Now we have

a conformal map projection of the negatively curved  $k = -1$  universe onto a plane. This conformal map is the one illustrated in Escher’s famous angels and devils print which is often used to illustrate this cosmology (cf. Gott (2001)). Next we take this conformal planar map  $(r, \theta)$  and apply our conformal logarithmic mapping function to it. Thus, we produce a conformal map of the universe with coordinates:

$$x = -\theta \tag{A21}$$

$$y = \ln \frac{2a(t_0) \tanh(\chi/2)}{r_E} \tag{A22}$$

Note the similarity with the formula for a spherical  $k = +1$  universe; in the  $k = -1$  case “tanh” simply replaces “tan”.

We can make maps for all three cases. These are useful for comparison purposes. For example suppose we develop an isotropy measure for voids as suggested by Barbara Ryden. We could apply this to the voids on our conformal universe map since it preserves shapes locally and the voids are small. The shapes of the voids depend on the assumed cosmological model. This is the Alcock–Paczynski test. If we have the right cosmological model the voids will be approximately round as suggested by Ryden, and this can be tested. Suppose, as WMAP suggests, the flat  $k = 0$  case is correct with  $\Omega_m + \Omega_\Lambda = 1$ , Then we can plot the same redshift data but conformally assuming slightly closed  $\Omega_m + \Omega_\Lambda > 1$ ,  $k = +1$  models or slightly open  $\Omega_m + \Omega_\Lambda < 1$ ,  $k = -1$  models and check isotropy of the voids in each case. We can thus check how sensitive the isotropy test is in limiting the location of the model in the  $(\Omega_m, \Omega_\Lambda)$  parameter plane.

## B. Sources

In applying the logarithmic map to the problem of showing the Universe, we have used a multitude of both online sources, personal communication and data published in journals. To illustrate the wealth and variety of data depicted in the Map, we have chosen to list the sources in this section.

- Moon phase  
United States Naval Observatory Astronomical Almanac, (USNO Almanac (2003))  
( <http://aa.usno.navy.mil/data/docs/MoonPhase.html> )
- Earth geological data  
Allen’s Astrophysical Quantities (Cox (2000))

- Artificial satellites

Mike McCants' Satellite Tracking web pages (alldat.tle file). The file includes orbital elements supplied by OIG (NASA/GSFC Orbital Information Group) and data on other satellites obtained primarily by amateur visual observations.

( <http://oig1.gsfc.nasa.gov/> )

( <http://users2.ev1.net/~mmccants/tles/index.html> )

- Hubble Space Telescope location

Alan Patterson & Davin Workman (Science and Mission Scheduling Branch, Operations and Data Management Division, Space Telescope Science Institute), private communication

- Chandra X-ray Observatory location

Rob Cameron (CXO Science Operations Team), private communication

- Asteroid catalog

Lowell Observatory Asteroid Database (ASTORB), 2003/04/19 snapshot, with ephemeris calculated for Aug 12, 2003

<ftp://ftp.lowell.edu/pub/elgb/astorb.html>

- Minor bodies' ephemeris

Ephemeris computed using an adapted version of the OrbFit software package.

OrbFit is written by the OrbFit consortium: Dept. of Mathematics, Univ. of Pisa (Andrea Milani, Steven R. Chesley), Astronomical Observatory of Brera, Milan (Mario Carpinò), Astronomical Observatory, Belgrade (Zoran Knežević), CNR Institute for Space Astrophysics, Rome (Giovanni B. Valsecchi).

( <http://newton.dm.unipi.it/~neodys/astinfo/orbfit/> )

- Quaoar and Sedna information

( <http://www.gps.caltech.edu/~chad> )

- Comet, Sun, Moon and planet ephemeris

Generated using JPL HORIZONS On-line Solar System Data and Ephemeris Computation Service.

( <http://ssd.jpl.nasa.gov/horizons.html> )

- Space probes

Voyager 1, Voyager 2, Pioneer 10, Ulysses positions obtained from NASA HeliWeb webpage at NSSDC (National Space Science Data Center)

( <http://nssdc.gsfc.nasa.gov/space/helios/heli.html> )

- Heliopause

Distance taken to be approximately 110 AU in the direction of approximately 18h RA.

- Oort Cloud

Taken to extend from 8,000 AU to 100,000 AU

- 10 brightest stars

Source for positions and parallaxes: SIMBAD Reference database, Centre de Donnees astronomiques de Strasbourg

( <http://simbad.u-strasbg.fr/sim-fid.pl> )

- 10 nearest stars

Source for positions and parallaxes: Research Consortium on Nearby Stars, list as of July 1, 2004

( <http://www.chara.gsu.edu/RECONS/TOP100.htm> )

- Extra-solar planets

IAU “Working Group on Extrasolar Planets” list of planets, the ”Extrasolar Planets Catalog” of the ”Extrasolar Planets Encyclopedia” maintained by Jean Schneider at CNRS – Paris Observatory

( <http://www.ciw.deu/IAU/div3/wgesp/planets.shtml> )

( <http://www.obspm.fr/encycl/encycl.html> )

( <http://cfa-www.harvard.edu/planets/OGLE-TR-56.html> )

- Hipparcos stars

ESA, 1997, The Hipparcos and Tycho Catalogues, ESA SP-1200

( <http://tdc-www.harvard.edu/software/catalogs/hipparcos.html> )

- Selected Messier objects

Distances and common names taken from the Students for the Exploration and Development of Space (SEDS) Messier Catalog pages. Positions taken from the SIMBAD reference database

( <http://www.seds.org/messier/> )

- Milky Way

Disk radius taken to be 15kpc. Distance to galactic center taken to be 8kpc.

- Local Group

Data taken from a list of Local Group Member Galaxies maintained by SEDS

( <http://www.seds.org/~spider/spider/LG/lg.html> )

- Great Attractor  
Location data from SIMBAD, redshift distance:  $cz = 4,350 \text{ km s}^{-1}$
- Great Wall  
Contours based on CfA2 redshift Catalog, subset CfA2. The contours are based on galaxies satisfying  $-8.5^\circ < \delta < 42.5^\circ$ ,  $120^\circ < \alpha < 255^\circ$ , and  $0.01 < z < 0.05$  comprising the CfA2's first 6 slices (Geller and Huchra (1989)).  
( <http://cfa-www.harvard.edu/~huchra> )
- SDSS data  
Plotted from raw SDSS spectroscopy data obtained using David Schlegel's SPECTRO pipeline – spALL.dat file – dated 2003/01/15 with a  $z < 5$  inclusion cut applied.  
SDSS quasar data with  $z > 5$  provided by Michael Strauss, private communication.  
( <http://spectro.princeton.edu/> )
- Plotting  
Plotted using SM software by Robert H. Lupton.  
( <http://astro.princeton.edu/~rhl/sm> )
- Individual quasar data  
SIMBAD database
- Cosmological data  
WMAP Collaboration publications ( Bennett et al. (2003) )
- WMAP location in space at the time of the map  
Dale Fink, Gary Hinshaw, Hiranya Peiris (2003), personal communication

## REFERENCES

- K. Abazajian, AJ, in press, astro-ph/0305492 (2003)
- Alcock C., Paczynski B., 1979, Nature, 281, 358
- Alonso, R., et al. 2004, ApJ, 613, L153
- Bahcall, N. A. & Soneira, R. M. 1984, ApJ, 277, 27
- Belbruno, E., & Gott, J. R., astro-ph/0405372 (2004)
- Bennett, C. L. et al. 2003, ApJS, 148, 1

- Blanton, M. R. et al. 2003, ApJ, 592, 819
- Blanton, M.R., Lupton, R.H., Maley, F.M., Young, N., Zehavi, I., and Loveday, J. 2003, AJ, 125, 2276
- Boeke, K., Cosmic View: The Universe in 40 Jumps, John Day Company, New York (1957)
- Bond, I. A., et al. 2004, ApJ, 606, L155
- Brown, M. E., Trujillo, C. A., & Rabinowitz, D. L. 2004, IAU Circ., 8304, 1
- Michael T. Busha, Fred C. Adams, Risa H. Wechsler, and August E. Evrard, 2003, ApJ, 596, 713
- Cole, S., Hatton, S., Weinberg, D. H., & Frenk, C. S. 1998, MNRAS, 300, 945
- Colless, M. et al. 2001, MNRAS, 328, 1039
- Colley, W. N., Gott, J. R. I., Weinberg, D. H., Park, C., & Berlind, A. A. 2000, ApJ, 529, 795
- Connors, M., et al. 2002, M&PS, 37, 1435 (2002)
- Connors, M., et al., 35th Lunar and Planetary Science Conference, March 15-19, 2004, League City, Texas, abstract no.1565
- Cox, A. N., Allen's Astrophysical Quantities, 4th edition, AIP press, Springer (2000)
- Croft, R. A. C., Weinberg, D. H., Bolte, M., Burles, S., Hernquist, L., Katz, N., Kirkman, D., & Tytler, D. 2002, ApJ, 581, 20
- de Lapparent, V., Geller, M. J., & Huchra, J. P. 1986, ApJ, 302, L1
- De Peyng, R., Amoco Map of Space Mysteries (1958)
- Eames, C. and Eames, R., Powers of Ten (Movie—9.5 minutes), Office of Charles and Ray Eames for IBM (1977)
- Eisenstein, D. J. et al. 2001, AJ, 122, 2267
- ESA, 1997, The Hipparcos and Tycho Catalogues, ESA SP-1200
- Freedman, W. L. et al. 2001, ApJ, 553, 47
- Fukugita, M., Ichikawa, T., Gunn, J. E., Doi, M., Shimasaku, K., & Schneider, D. P., AJ, 111, 1748 (1996)

- Garnavich, P. M. et al. 1998, ApJ, 509, 74
- J. Garriga and A. Vilenkin, Phys. Rev. D 57, 2230 (1998)
- Geller, M. and Huchra, J., Science, 246, 897 (1989)
- Gnedin, N. Y. & Hamilton, A. J. S. 2002, MNRAS, 334, 107
- Krzysztof M. Górska, Eric Hivon, Benjamin D. Wandelt, astro-ph/9812350 (1998)
- Gott, J.R., Time Travel in Einstein's Universe, p 175, Houghton Mifflin, New York, 2001.
- Gott, J. R., Dickinson, M., & Melott, A. L. 1986, ApJ, 306, 341
- Gunn, J. E., et al., AJ, 116, 3040 (1998)
- Henry G., Marcy G., Butler P. & Vogt S., IAU telegram 7307, (1999)
- Hikage, C. et al. 2002, PASJ, 54, 707
- Hogg, D. W., astro-ph/9905116 (1999)
- Hogg, D.W., Finkbeiner, D.P., Schlegel, D.J., and Gunn, J.E. 2001, AJ, 122, 2129
- Hoyle, F. et al. 2002, ApJ, 580, 663
- Kaiser, N. 1987, MNRAS, 227, 1
- Kodaira, K. et al. 2003, PASJ, 55, L17
- Krauss, L. M. & Starkman, G. D. 2000, ApJ, 531, 22
- Kundic, T., et al. 1997, ApJ, 482, 75
- A. Linde, Particle Physics and Inflationary Cosmology (Harwood academic Publishers, Chur, Switzerland) (1990)
- Mazeh, T., et al. 2000, ApJ, 532, L55
- Morrison, P., Morrison, and the Office of Charles & Ray Eames, Powers of Ten, Scientific American Library, New York. 1982
- Park, C. 1990, MNRAS, 242, 59P
- Penzias, A. A. & Wilson, R. W. 1965, ApJ, 142, 419
- Percival, W. J. et al. 2001, MNRAS, 327, 1297

- Perlmutter, S. et al. 1999, ApJ, 517, 565
- Pier, J. R., Munn, J. A., Hindsley, R. B., Hennessy, G. S., Kent, S. M., Lupton, R. H., & Ivezić, Ž. 2003, AJ, 125, 1559
- Praton, E. A., Melott, A. L., & McKee, M. Q. 1997, ApJ, 479, L15
- Richards, G. T. et al. 2002, AJ, 123, 2945
- Riess, A. G. et al. 2001, ApJ, 560, 49
- Ryden, B. S. 1995, ApJ, 452, 25
- Ryden, B. S. & Melott, A. L. 1996, ApJ, 470, 160
- Schmidt M., 1963, Nature, 197, 1040
- J.C. Slater, J. Chem. Phys. 39, 3199 (1964)
- Sloan, C., Fierstein, D., Gott, J. R., Hayes, J., Osserman, R., Weeks, J., The view from Earth (Map), National Geographic, October (1999)
- Smith, J.A., et al 2002, AJ, 123, 2121
- Smoot, G. F. et al. 1992, ApJ, 396, L1
- Snyder, J. P., Flattening the Earth, University of Chicago Press, Chicago (1993)
- Spergel, D. N. et al. 2003, ApJS, 148, 175
- Steinberg, S., “View of the World from 9th Avenue”, New Yorker Cover, May 29, 1976
- Stoughton, C., et al 2002, AJ, 123, 485
- Strauss, M. A. et al. 2002, AJ, 124, 1810
- Teegarden, B. J., et al. 2003, ApJ, 589, L51
- Turner, E. L. and Gott, J. R., Ap.J. Supplement, 32, 409 (1976)
- United States Naval Observatory Astronomical Almanac, 2003
- Verde, L. et al. 2002, MNRAS, 335, 432
- Vogeley, M. S., Park, C., Geller, M. J., Huchra, J. P., and Gott, J. R., Ap.J., 420, 525 (1994)
- Wolszczan, A. 1994, Science, 264, 538

Wolszczan, A. & Frail, D. A. 1992, Nature, 355, 145

York, D. G., et al., AJ, 120, 1579 (2000)

Table 1. Co-moving radii for different redshifts

$z$	$r(z)$ (Mpc)	Note
$\infty$	14,283	Big Bang (end of inflationary period)
3233	14,165	Equal matter and radiation density epoch
1089	14,000	Recombination
6	8,422	
5	7,933	
4	7,305	
3	6,461	
2	5,245	
1	3,317	
0.5	1,882	
0.2	809	
0.1	413	

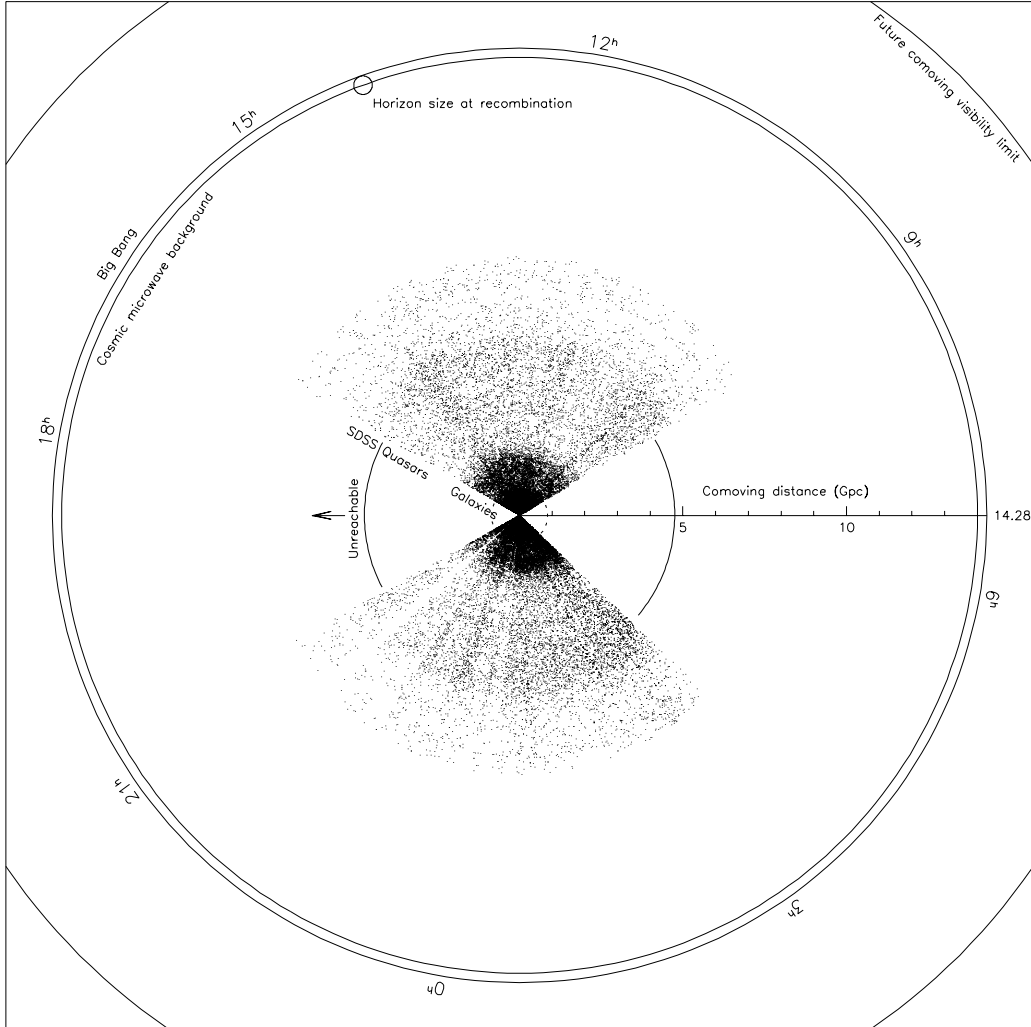


Fig. 1.— Galaxies and quasars in the equatorial slice ( $-2^\circ < \delta < 2^\circ$ ) of the Sloan Digital Sky Survey displayed in co-moving coordinates out to the horizon. The co-moving distances to galaxies are calculated from measured redshift, assuming Hubble flow and WMAP cosmological parameters. This is a conformal map – it preserves shapes. While this map can conformally show the complete Sloan survey, the majority of interesting large scale structure is crammed into a blob in the center. The dashed circle marks the outer limit of figure 2. The circle labeled 'Unreachable' marks the distance beyond which we cannot reach (i.e. we cannot reach with light signals any object that is further away). This radius corresponds to a redshift of  $z = 1.69$ . As 'Future comoving visibility limit' we label the co-moving distance to which a photon would travel from the inflationary Big Bang to the infinite future. This is the maximum radius out to which observations will ever be possible. At  $4.50R_{H_0}$ , it is surprisingly close.

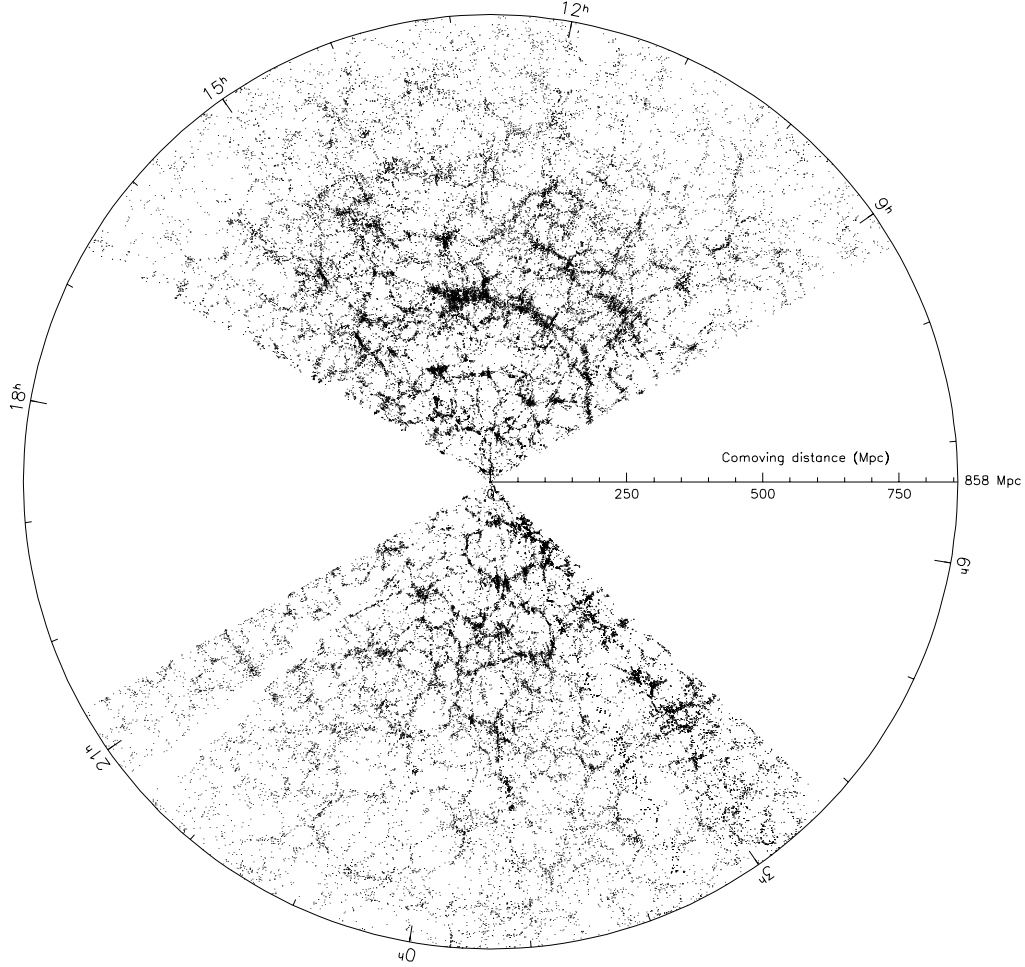


Fig. 2.— Zoom in of the region marked by the dashed circle in figure 1, out to  $0.06 r_{\text{horizon}}$  ( $= 858 \text{ Mpc}$ ). The points shown are galaxies from the main and bright red galaxy samples of the SDSS. Compared to figure 1, we can now see a lot of interesting structure. The Sloan Great Wall can be seen stretching from  $8.7\text{h}$  to  $14\text{h}$  in R.A. at a median distance of about  $310 \text{ Mpc}$ . Although the large scale structure is easier to see, a "zoom in" like this fails to capture and display, in one map, the sizes of modern redshift surveys.

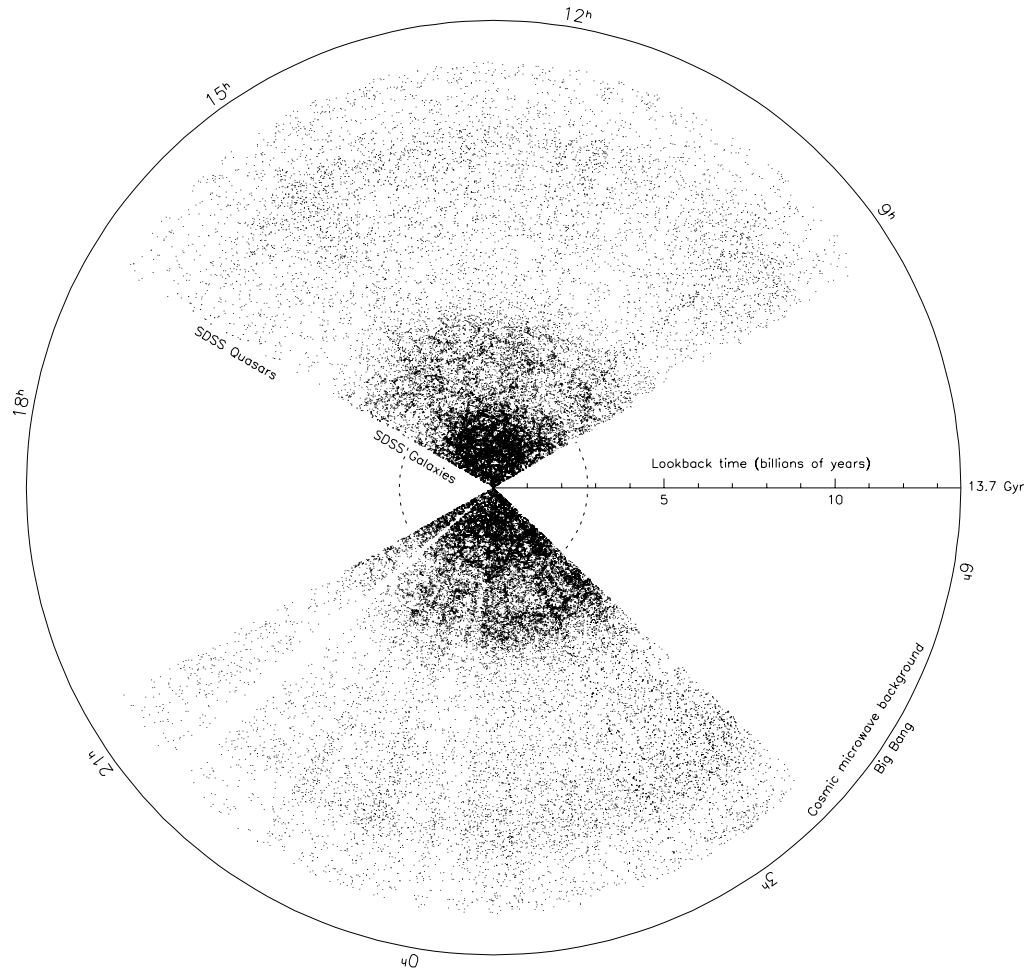


Fig. 3.— Galaxies and quasars in the equatorial slice of the SDSS, displayed in lookback time coordinates. The radial distance in the figure corresponds to lookback time. While the Galaxies at the center occupy a larger area, this map is a misleading portrayal as far as shapes and the geometry of space are concerned. It is not conformal – it compresses the area close to the horizon (this compression is more explicitly shown in figure 5). Also, the galaxies are still too crowded in the center of the map to show all of the intricate details of their clustering. Figure 4 shows a zoom in of the region inside the dashed circle.

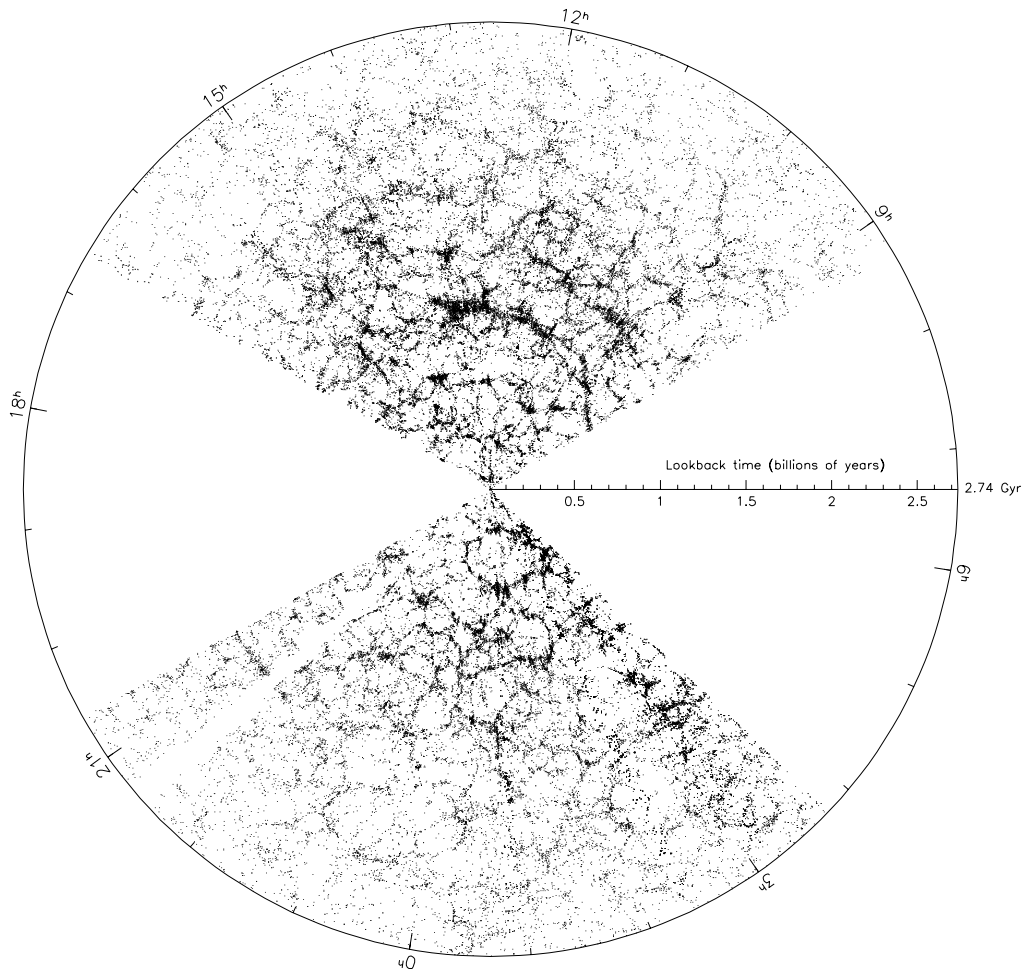


Fig. 4.— Zoom in of the region marked by the dotted circle in figure 3, showing SDSS galaxies out to  $0.2 t_{\text{horizon}}$ . The details of galaxy clustering are now displayed much better. However, like figure 2, it still fails to capture the whole survey in one, reasonably sized, map.

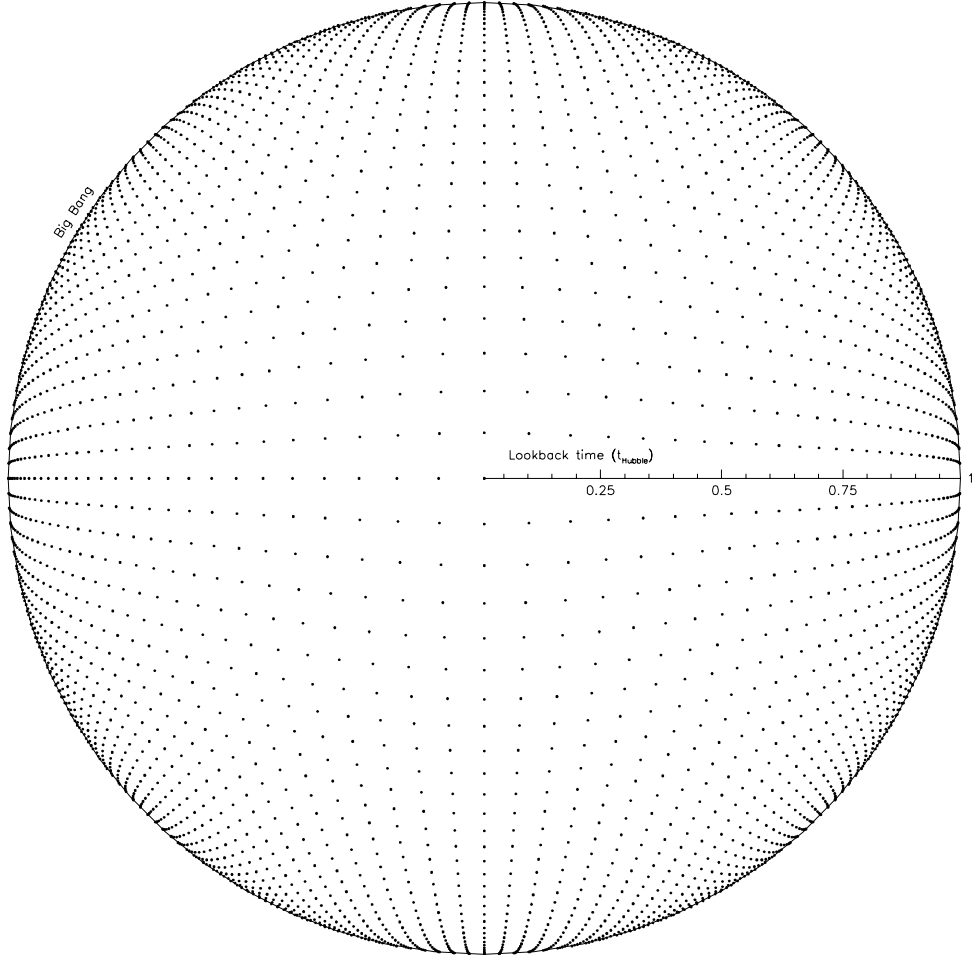


Fig. 5.— Square comoving grid shown in lookback time coordinates. Grid spacing is  $0.1R_{H_0} = 422.24$  Mpc. Each grid square would contain an equal number of galaxies in a flat slice of constant vertical thickness. The distortion of space that is produced by using the lookback time is obvious as the squares become more and more distorted in shape as one approaches the horizon.

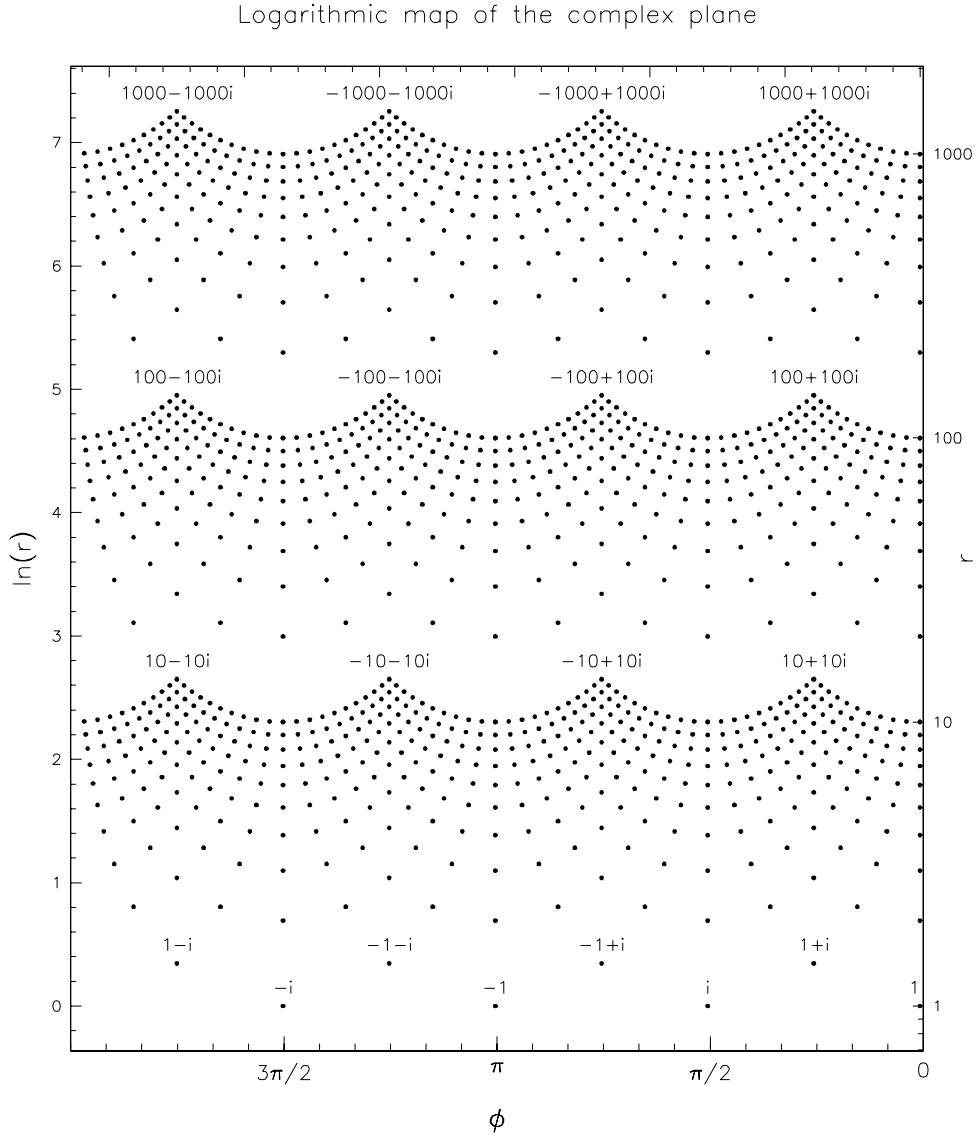


Fig. 6.— Logarithmic map of the complex plane. Vertical axis is the natural logarithm of the absolute value of a complex number, while its phase is plotted on the horizontal axis. We plot  $4 \times 10 \times 10$  numbers per decade, from the first three decades. This map is conformal, but covers a wide range of scales.

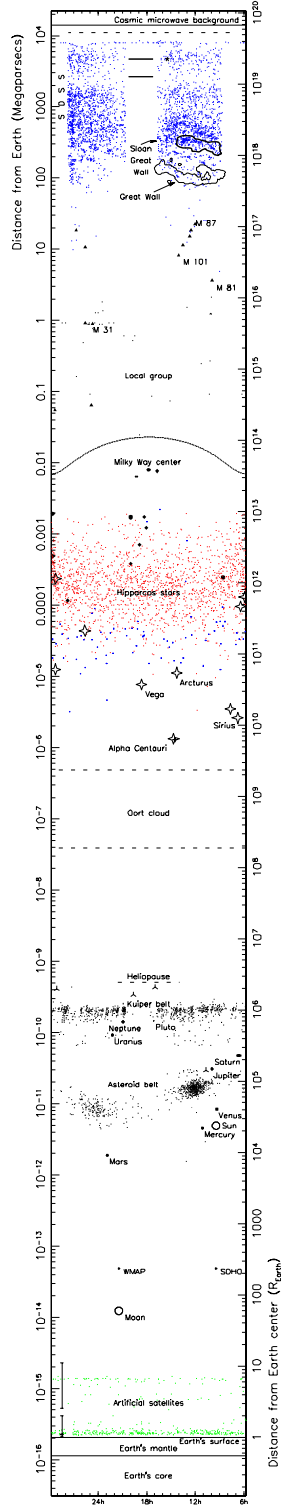


Fig. 7.— Pocket map of the universe. A smaller version of the more detailed map shown in the foldout figure 8

Fig. 8.— Map of the Universe. This figure is available separately from  
<http://www.astro.princeton.edu/~mjuric/universe>

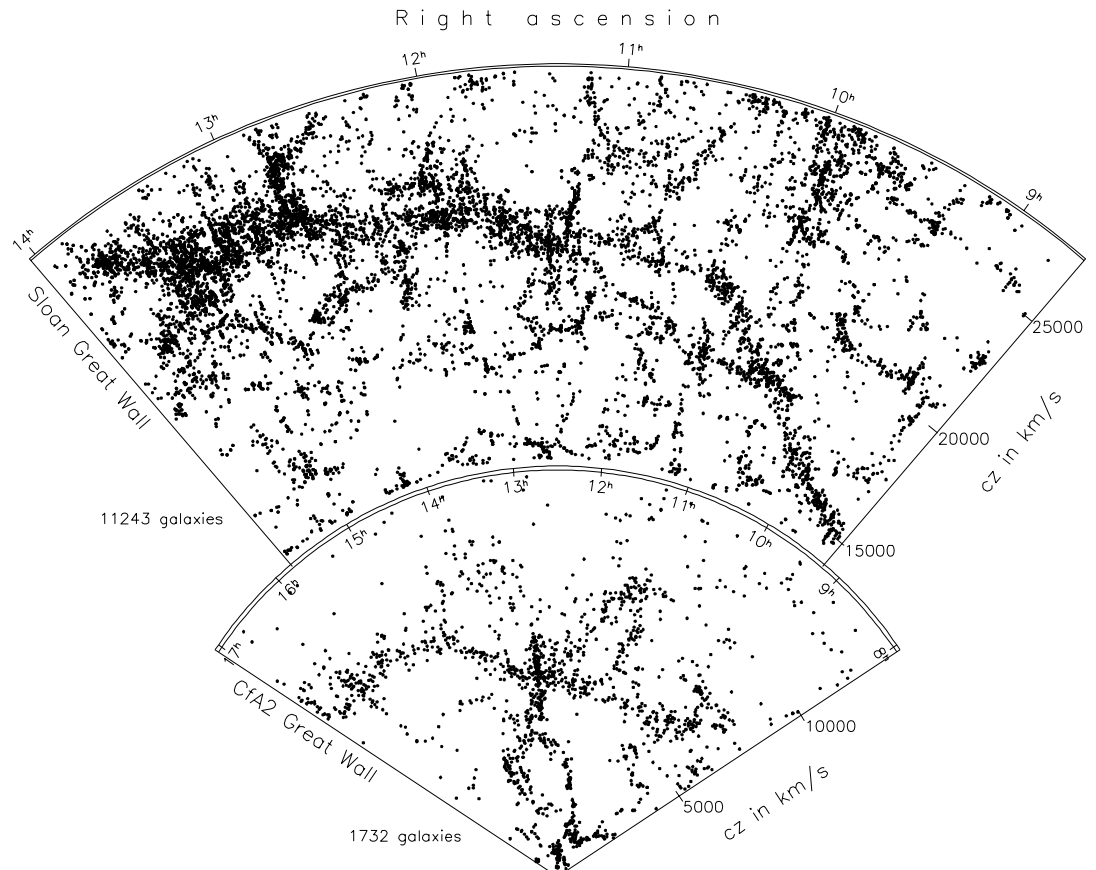


Fig. 9.— Sloan Great Wall compared to CfA2 Great Wall at the same scale in co-moving coordinates. Equivalent redshift distances  $cz$  are indicated. The Sloan slice is  $4^\circ$  wide, the CfA2 slice is  $12^\circ$  wide to make both slices approximately the same physical width at the two walls. The Sloan Great Wall extends from  $14h$  to  $9h$ . It consists of one strand at the left, which divides to form two strands between  $11.3h$  and  $9.8h$ , which come back together to form one strand again (like a road that becomes a divided highway for a while). The CfA2 Great Wall (which includes the Coma cluster in the center), has been plotted on a cone and then flattened onto a plane. Total numbers of galaxies shown in each slice are also indicated.